AD-A171 450 THE RELATIONSHIP BETWEEN MICROMETEOROLOGY AND SOUND 1/1
PROPAGATION ABOVE SNO (U) PENNSYLVANIA STATE UNIV
UNIVERSITY PARK O W MCDANIEL ET AL 15 JUN 86
UNCLASSIFIED ARO-21498.2-GS DAAG29-84-K-0085 F/G 20/1 NL

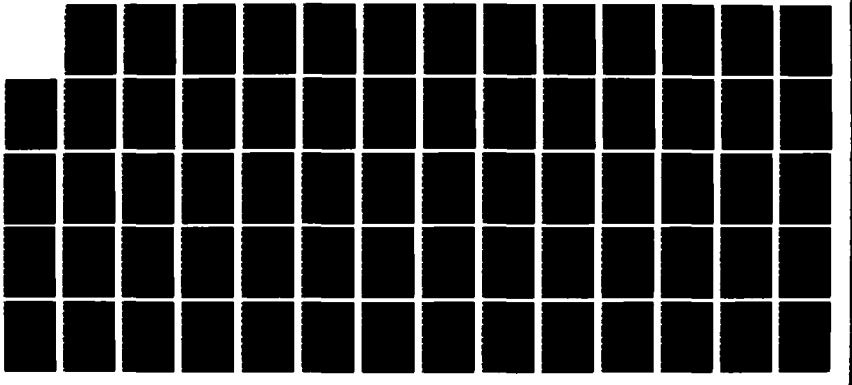

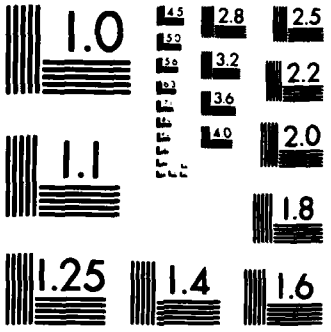

MICROCOPY RESOLUTION TEST CHART
NATIONAL BUREAU OF STANDARDS-1963-A

The Relationship Between Micrometeorology and Sound Propagation above Snow-covered and Ground Surfaces

Final Report

Oliver H. McDaniel
Dennis W. Thomson

15 June 1986

U.S. Army Research Office
P. O. Box 12211
Research Triangle Park, NC 27709

Contract No. DAAG 29-84-K-0085

The Pennsylvania State University
University Park, PA 16802

UNCLASSIFIED

SECURITY CLASSIFICATION OF THIS PAGE (When Data Entered)

REPORT DOCUMENTATION PAGE		READ INSTRUCTIONS BEFORE COMPLETING FORM
1. REPORT NUMBER ARO 21498.2-GS	2. GOVT ACCESSION NO. N/A	3. RECIPIENT'S CATALOG NUMBER N/A
4. TITLE (and Subtitle) The Relationship Between Micrometeorology and Sound Propagation above Snow-covered and Ground Surfaces		5. TYPE OF REPORT & PERIOD COVERED Final July 1, 1984 to June 30, 1985 6. PERFORMING ORG. REPORT NUMBER
7. AUTHOR(s) Oliver H. McDaniel Dennis W. Thomson		8. CONTRACT OR GRANT NUMBER(s) DAAG-29-84-K-0085
9. PERFORMING ORGANIZATION NAME AND ADDRESS The Pennsylvania State University University Park, PA 16802		10. PROGRAM ELEMENT, PROJECT, TASK AREA & WORK UNIT NUMBERS
11. CONTROLLING OFFICE NAME AND ADDRESS U. S. Army Research Office Post Office Box 12211 Research Triangle Park, NC 27709		12. REPORT DATE 13. NUMBER OF PAGES
14. MONITORING AGENCY NAME & ADDRESS(if different from Controlling Office)		15. SECURITY CLASS. (of this report) Unclassified 15a. DECLASSIFICATION/DOWNGRADING SCHEDULE

16. DISTRIBUTION STATEMENT (of this Report)

Approved for public release; distribution unlimited.

17. DISTRIBUTION STATEMENT (of the abstract entered in Block 20, if different from Report)

NA

18. SUPPLEMENTARY NOTES

The view, opinions, and/or findings contained in this report are those of the author(s) and should not be construed as an official Department of the Army position, policy, or decision, unless so designated by other documentation.

19. KEY WORDS (Continue on reverse side if necessary and identify by block number)

Atmospheric sound propagation, meteorology, acoustics, snow cover.

20. ABSTRACT (Continue on reverse side if necessary and identify by block number)

This report summarizes measurements of sound at 24 non-harmonically related frequencies which were simultaneously transmitted over the same snow-covered and bare ground over 30, 60 and 120 m paths. Eleven frequencies each were transmitted at $\simeq$ 1/2 and 2 m height and were received on microphones positioned at the same heights at each distances. The measurements above snow were recorded on 1 and 2 February 1984, and above bare gound on a synopitically similar (from a wind speed, etc., point-of-view) day, the 26th of April, 1984. Simultaneously,

DD FORM 1 JAN 73 1473 EDITION OF 1 NOV 65 IS OBSOLETE

UNCLASSIFIED

SECURITY CLASSIFICATION OF THIS PAGE (When Data Entered)

a diverse set of micrometeorological measurements were recorded which would allow later analysis of the SL sound propagation medium.

The multi-tone transmitters, microphone receivers and recorder were operated a total of 225 min on the 1st and 2nd of February. A total of 79 minutes of measurements were logged on 26 April. On the basis of the analyzed micro-meteorological records, the time period 13:55 - 14:18 on 1 February and 13:56 - 14:19 on 26 April were chosen for initial "compare and contrast" purposes.

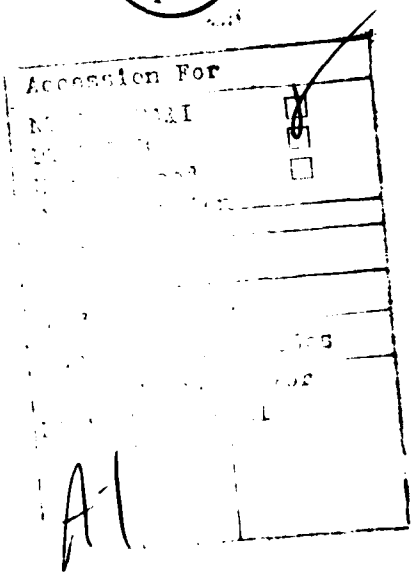

Acknowledgements

The authors wish to thank Richard Thompson, Robert Owens, Robert Peters and James Breon for thier able assistance in conducting the field measurements. We also wish to thank Harold Zintel, a Ph.D. candidate in the Penn State Graduate Program in Acoustics, for developing the data processing system and performing the statistical analysis and graphics presented in section 4b of this report.

Table of Contents

List of Figures

Page

List of Tables

1. Introduction

The characteristics of audible sound transmitted above the earth's surface depend not only upon the physical properties of the surface but also upon those of the overlying atmosphere. There have been many studies of outdoor sound propagation above vegetated surfaces (see, e.g., the review papers by Piercy, et al., 1977 and Delany, 1977). But there appear to be few published papers or measurements discussing aspects of sound propagation above snow (Watson, 1948; Tillotsen, 1965; Hasebe, 1983; Nicholas, et al., 1985). Furthermore, none of the above studies adequately examined the potential importance of the strong refractive index gradients which result from the combined temperature and velocity profiles which are characteristic of the atmosphere's surface layer (SL) above snow.

In contrast to the situation above vegetation in which the SL under clear sky and light to moderate wind conditions changes from being stably stratified (from infrared radiative cooling) at night to being convectively unstable (from solar heating during the day), the SL above snow often remains continuously stably stratified. More than 90% of the available sun's energy for heating can be "reflected" as a consequence of snow's high albedo. Of the remaining energy, some contributes to surface evaporation, much is absorbed beneath the surface and, thus, the maximum daytime temperatures in snow--which is also a poor thermal conductor--will occur several 10's of centimeters beneath the surface (see e.g., Oke, 1978). In short, the SL above snow will remain stably stratified throughout the day and at night. Since snow is "black" in the infrared, surface temperatures at night will drop to the minimum measured values.

The resulting strong SL temperature gradients not only produce beautiful optical mirages but also greatly alter the performance of a variety of EM

communications and surveilance systems. Furthermore, when the SL is stably stratified, wind velocity gradients will also be a maximum in the lower few meters. Hence, in the downwind direction the sound velocity or acoustic refractive index gradient in the SL will also be maximum.

In such a medium, will the characteristics of propagated audible sound or noise differ substantially from that observed above the same surface without snow? This report summarizes measurements of sound at 24 non-harmonically related frequencies which were simultaneously transmitted over the same snow covered and bare ground over 30, 60 and 120 m paths. Eleven frequencies each were transmitted at ≈ 1/2 and 2 m height and were received on microphones positioned at the same heights at each distance. The measurements above snow were recorded on 1 and 2 February 1984, and above bare ground on a synoptically similar (from a wind speed, etc., point-of-view) day, the 26th of April, 1984. Simultaneously, a diverse set of micrometeorological measurements were recorded which would allow later analysis of the SL sound propagation medium.

The multi-tone transmitters, microphone receivers and recorder were operated a total of 225 min on the 1st and 2nd of February. A total of 79 minutes of measurements were logged on 26 April. On the basis of the analyzed micro-meteorological records, the time periods 13:55-14:18 on 1 February and 13:56-14:19 on 26 April were chosen for initial "compare and contrast" purposes. Section four of this report includes illustrations of the cumulative probability distributions obtained from just one of each 23 minute sample from 1 February and 26 April at only 6 of the 24 recorded frequencies.

2. Meteorological Measurements

In the following figures, (a) in each case corresponds to 1 February, (b) to the 2nd and (c) to the 26th of April, respectively. Figure 1 illustrates the processed time series of solar radiation (labeled EPPLEY), the net radiation (labeled NETRAD) which defines the total energy available for evaporating water or ice, or heating the surface and the sensible atmospheric heat flux (labeled FLUX), $\rho c_p \overline{w'T'}$, where ρ is the density, c_p the specific heat and w' and T' are the vertical velocity and temperature fluctuations, respectively.

On 1 February, the sky was essentially clear, thus the smooth Eppley trace, and essentially all available solar radiation was reaching the surface. The flux density (W/m^2) was changing as a consequence of the varying elevation angle of the sun. Even at the solar maximum of nearly 600 W/m^2, the net radiation was only of order 20 W/m^2. At no time during the measurement period was the sensible heat flux positive, in other words the snow surface was constantly being warmed by the overlying air in which temperature was increasing with height. Unfortunately, the temperature probe amplifier was intermittent during the measurement period, and, thus, hand analysis of this data is still in progress. Figure 2 shows hourly temperature profiles recorded eleven days earlier during highly similar conditions. With the exception of the noon to 1300 hour average, which shows an approximately isothermal lapse rate, all profiles show an inversion to be present in the lowest 2 m. The sensible heat flux on the morning of 2 February was similar to that on the 1st, again indicating a flux of energy from the relatively warmer air in the SL temperature inversion to the snow surface. Further evidence to the absence of any "convective" type turbulence was provided by the recordings of the temperature structure parameter, C_T^2, from a path-averaging laser anemometer.

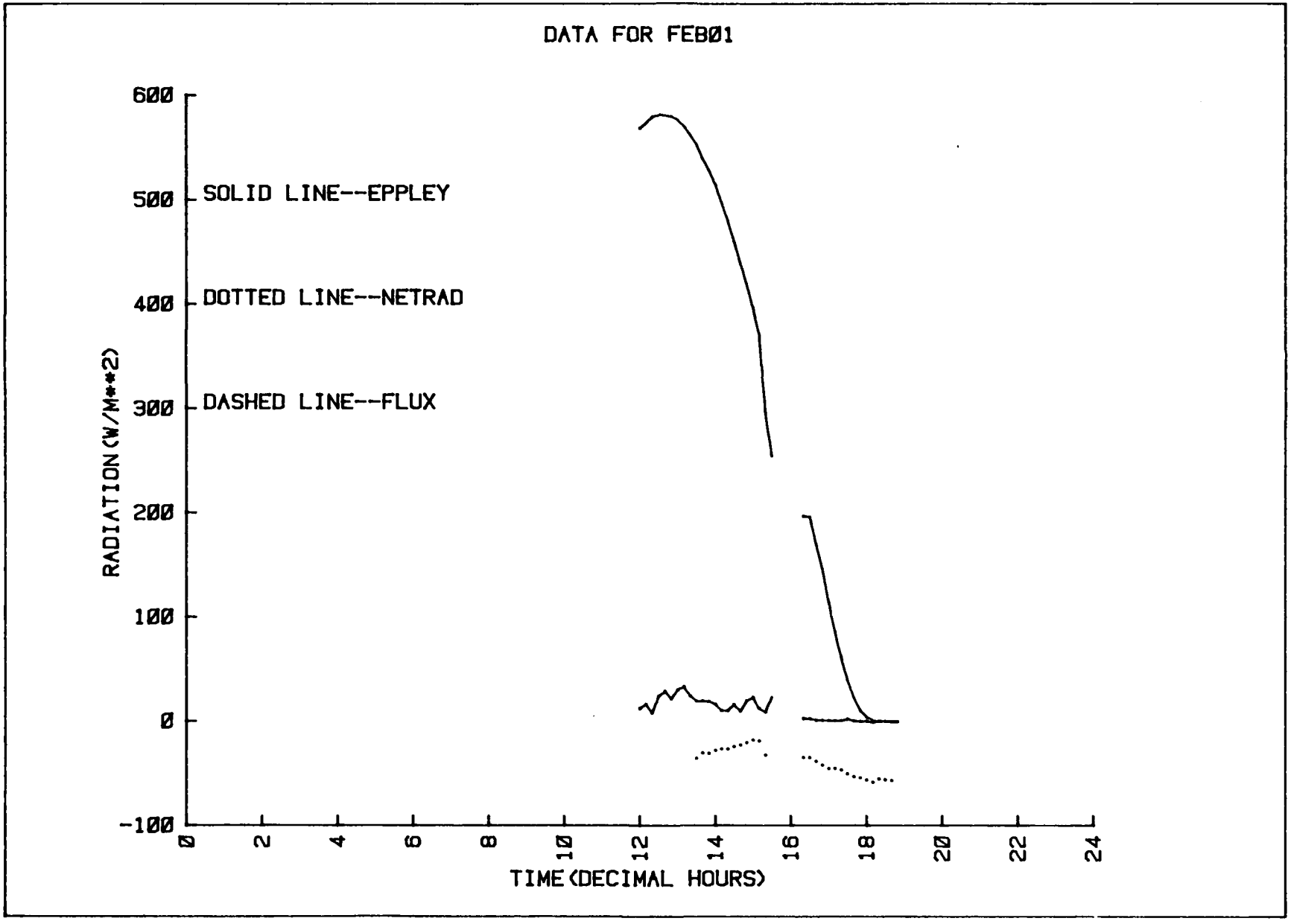

Figure 1a: Solar radiation, net radiation and sensible heat flux for 1 February 1984

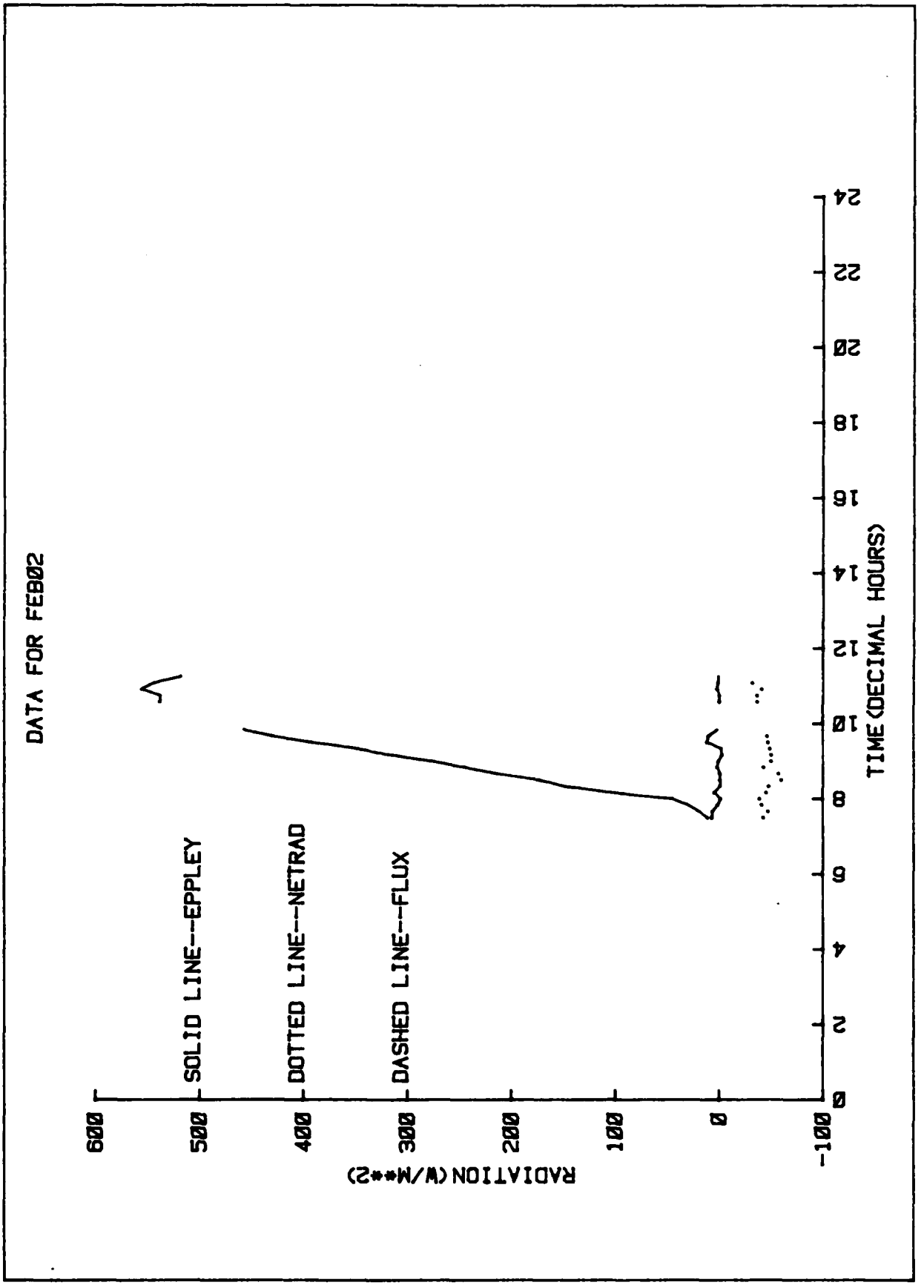

Figure 1b. Solar radiation and possible heat flux for 2 February 1984

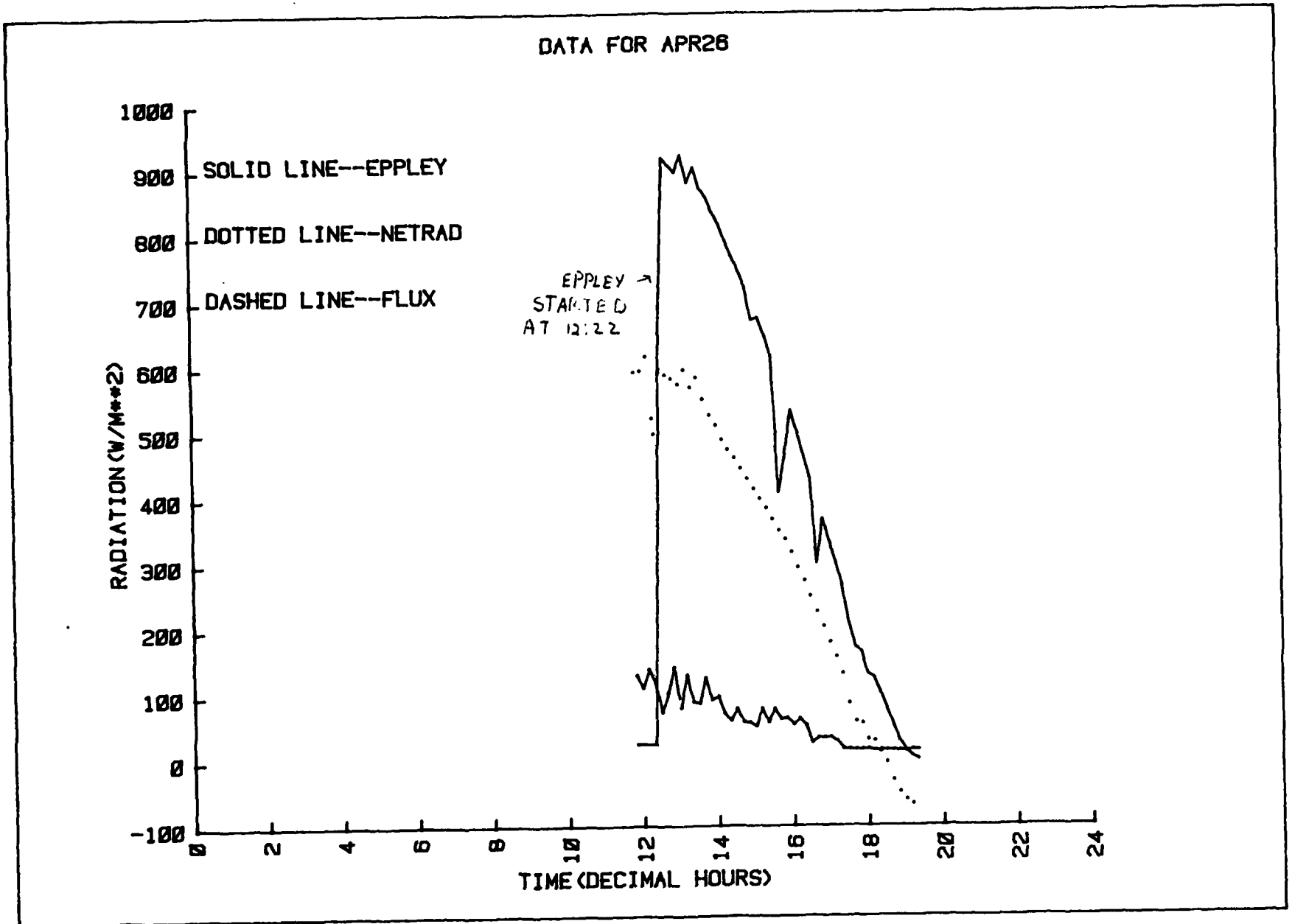
DATA FOR APR26
SOLID LINE--EPPLEY
DOTTED LINE--NETRAD
DASHED LINE--FLUX
EPPLEY STARTED AT 12:22
RADIATION (W/M**2)
1000
900
800
700
600
500
400
300
200
100
0
-100
0
2
4
6
8
10
12
14
16
18
20
22
24
TIME (DECIMAL HOURS)

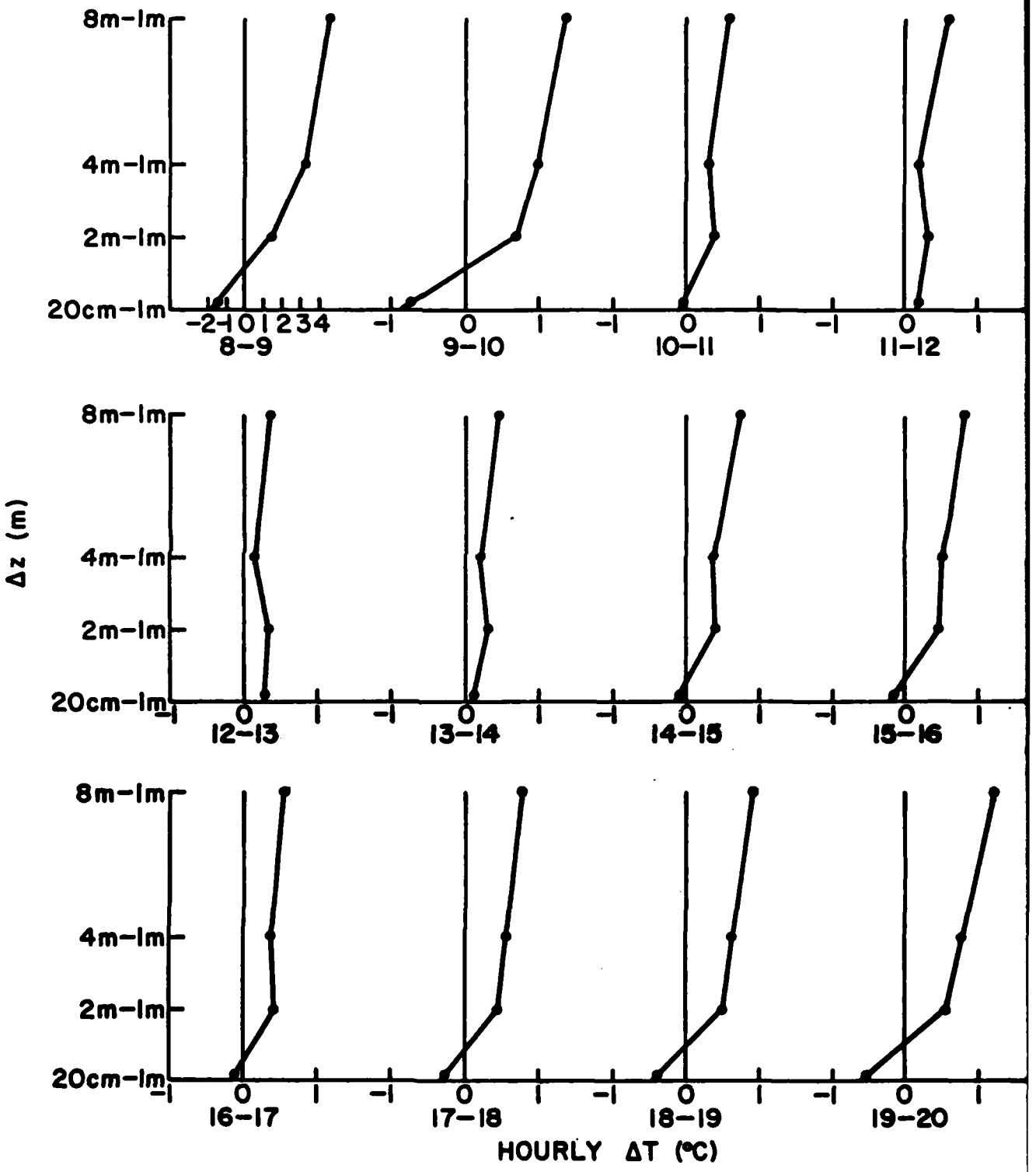

Figure 2: Hourly-averaged temperature profiles on 20 January 1984.

On both days the path averaged (300 m path parallel to the acoustic propagation path) C_T^2 was below threshold detection for the instrument. Visually, the laser signal was the steadiest we had ever observed.

On 26 April, a few bands of high cirriform clouds were present and thus some variability was evident in the Eppley trace (Figure 1c). The sensible heat flux was only about 15% of the net because the soil surface was relatively wet and, thus, most of the available radiant energy was being used for evaporating water. However, the sensible heat flux was positive and, thus, temperatures were decreasing with height in the SL until about 1700.

Light or calm winds (see Figure 2a, b and c) were one of the conditions for selecting the particular three measurement days. Furthermore, the days were chosen so that any winds present would be "up valley", that is orthogonal to the acoustic signal propagation path. In this manner it was hoped that any differences in the velocity gradient, and hence sound velocity gradient, resulting from differences in the aerodynamic roughness of the snow and ground surfaces would be minimized.

One meteorological variable over which we had no "experimental design" control was relative humidity. Since the absorption of sound is a function of frequency, relative humidity and temperature, the attenuation constant as a function of frequency and time was calculated for frequencies ranging from 63 to 8000 Hz for each day (Sutherland, et al., 1975). The purpose of these calculations was to assess the magnitude and natural variability of the attenuation constants (Figures 4a, b and c, 5a, b and c). Note that at 8000 Hz the short term variability is of order 1 to 2 dB/100 m and over one or two hours the change may be more than 10 dB/100 m.

It is also important to note that at frequencies less than 2 to 4 KHz, it is highly unlikely that any variability in received sounds, particularly

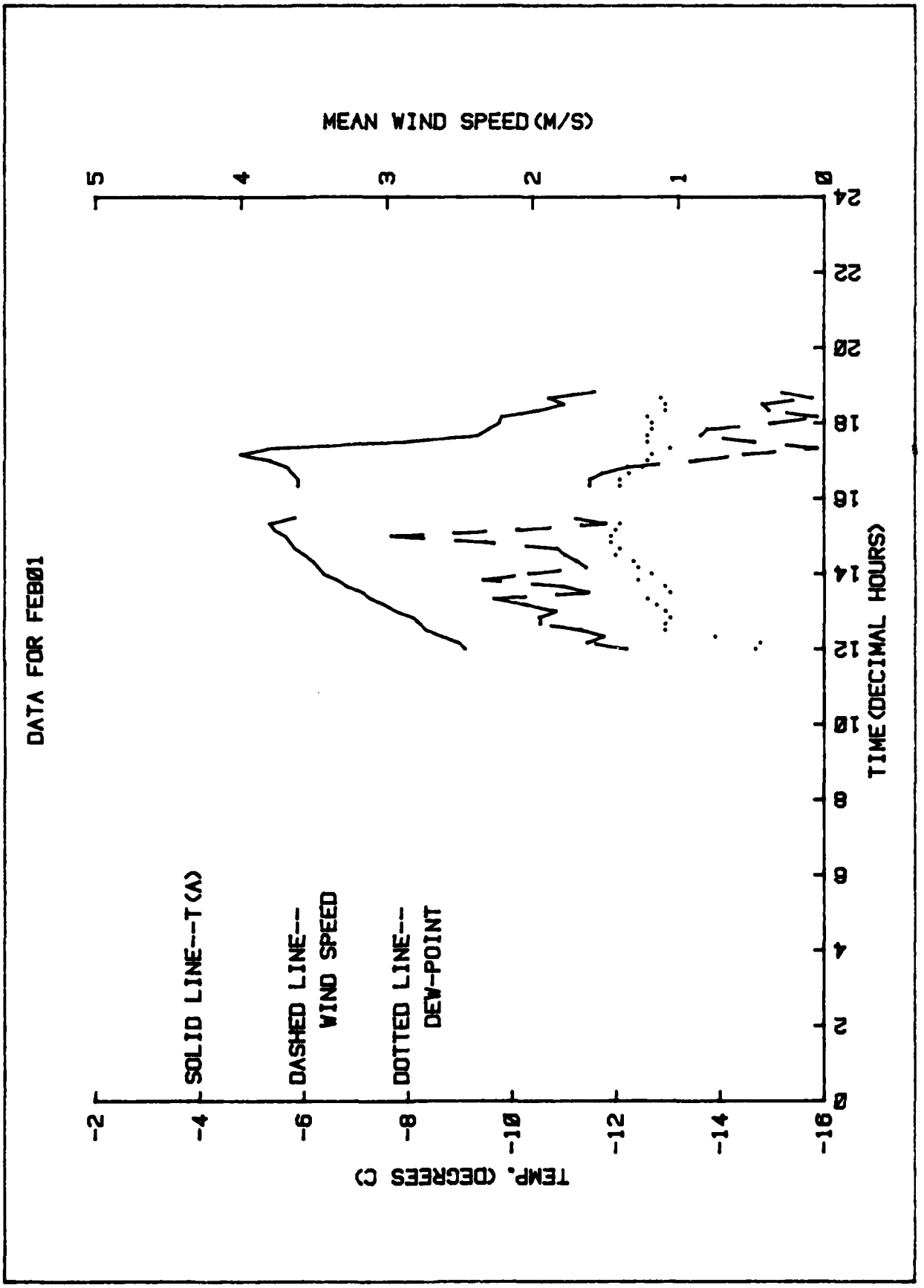
MEAN WIND SPEED (M/S)
5
4
3
2
1
0
24
22
20
18
16
14
12
10
8
6
4
2
0
TIME (DECIMAL HOURS)
DATA FOR FEB01
SOLID LINE--T(A)
DASHED LINE--
WIND SPEED
DOTTED LINE--
DEW-POINT
-2
-4
-6
-8
-10
-12
-14
-16
TEMP. (DEGREES C)

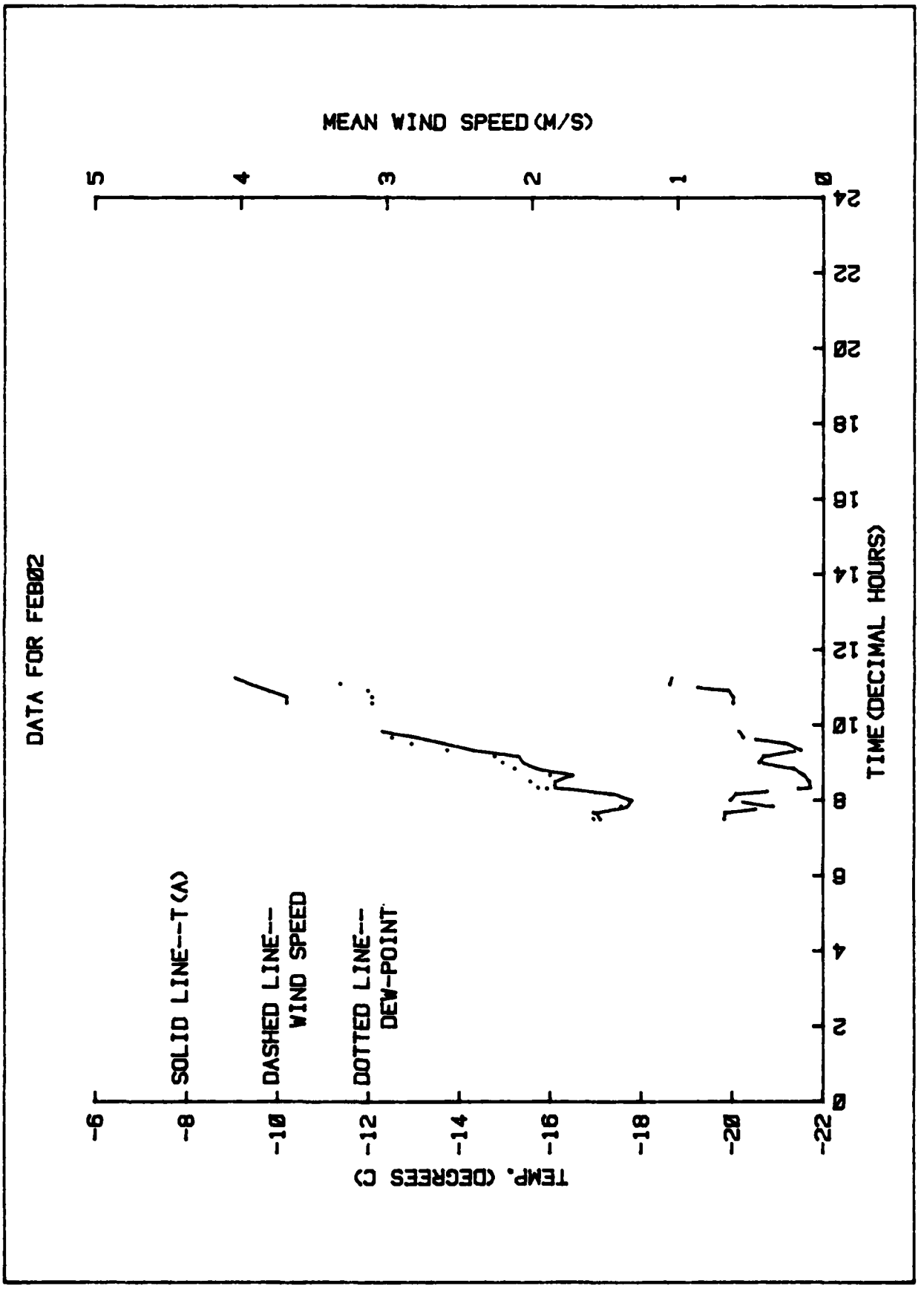
MEAN WIND SPEED (M/S)
5
4
3
2
1
0
24
22
20
18
16
14
12
10
8
6
4
2
0
TIME (DECIMAL HOURS)
DATA FOR FEB02
SOLID LINE--T(A)
DASHED LINE--
WIND SPEED
DOTTED LINE--
DEW-POINT
-6
-8
-10
-12
-14
-16
-18
-20
-22
TEMP. (DEGREES C)

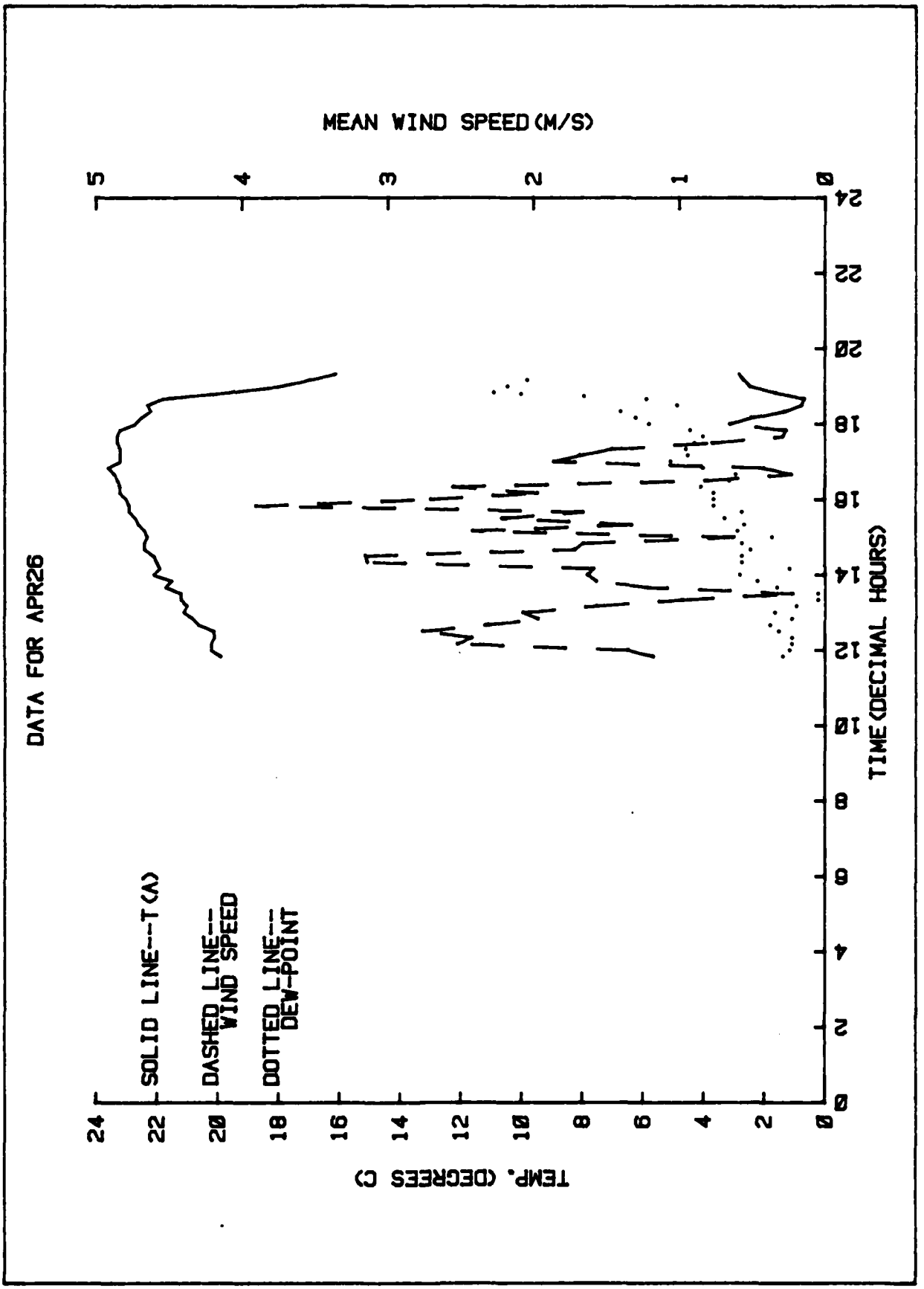
MEAN WIND SPEED (M/S)
5
4
3
2
1
0
24
22
20
18
16
14
12
10
8
6
4
2
0
TIME (DECIMAL HOURS)
TEMP. (DEGREES C)
DATA FOR APR26
SOLID LINE--T(A)
DASHED LINE--
WIND SPEED
DOTTED LINE--
DEW-POINT

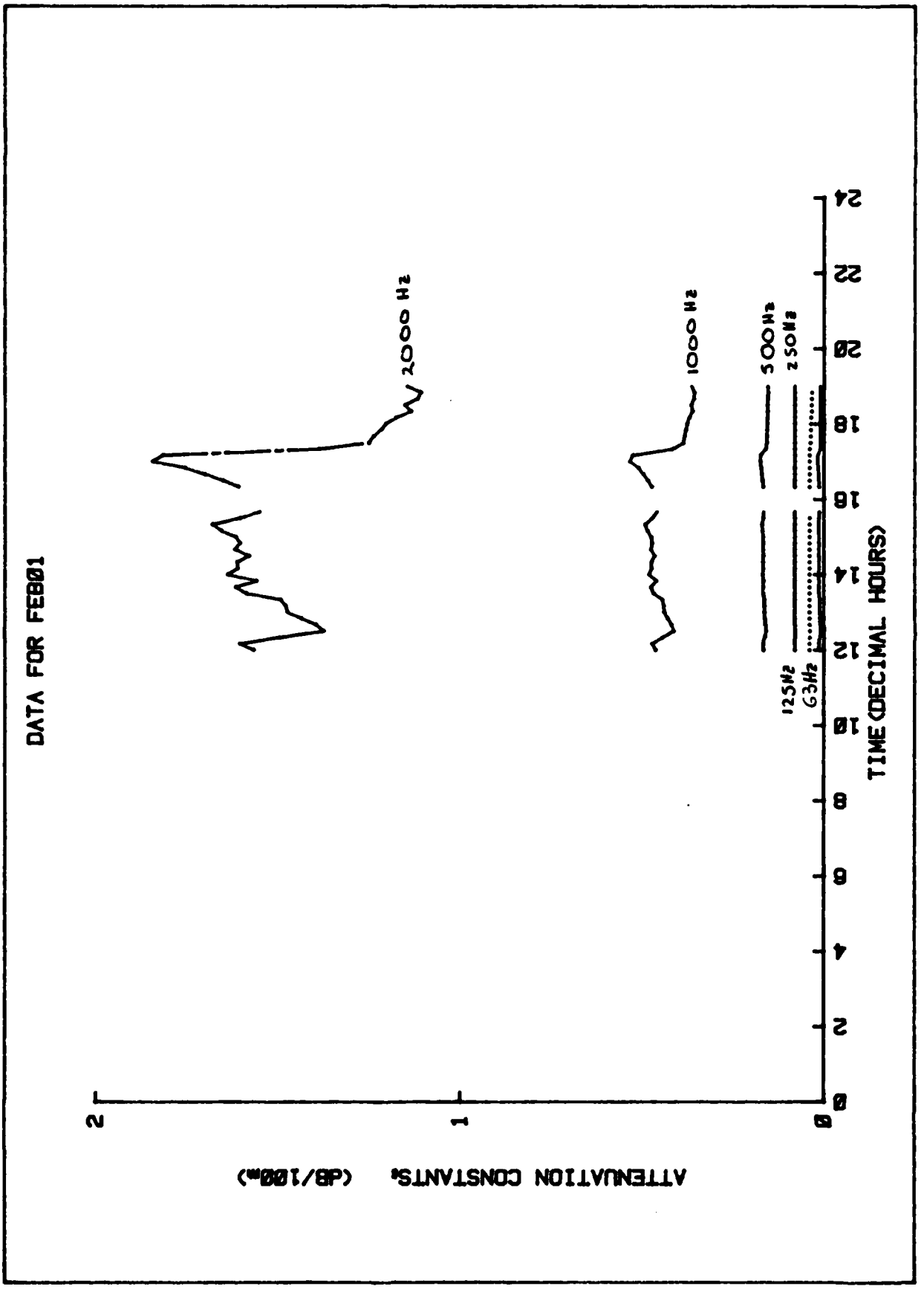

Figure 4a: Octave band attenuation constants at frequencies ranging from 63 to 2000 Hz

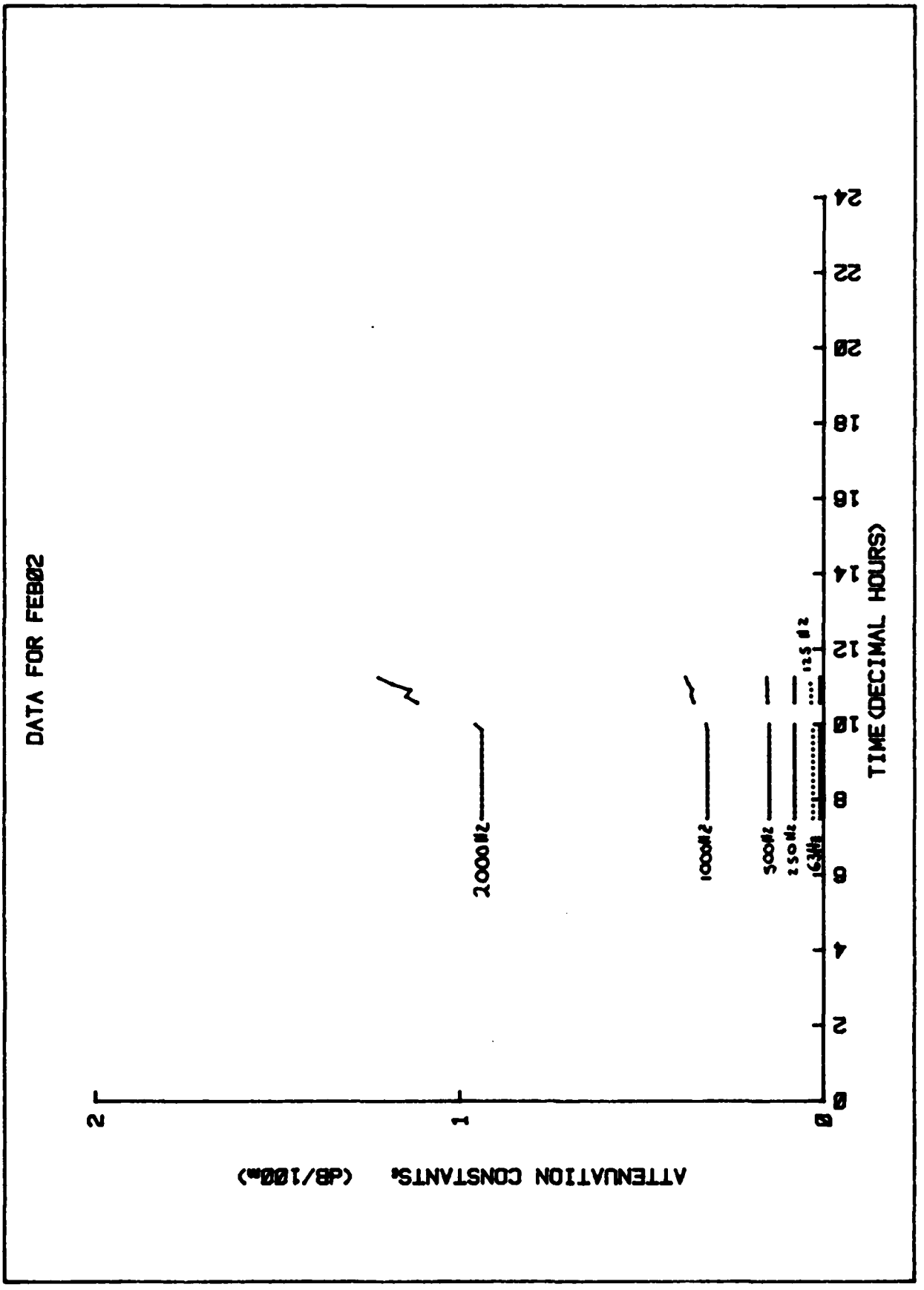

Figure 4b. Octave band attenuation constants at frequencies ranging from 63 to 2000 Hz

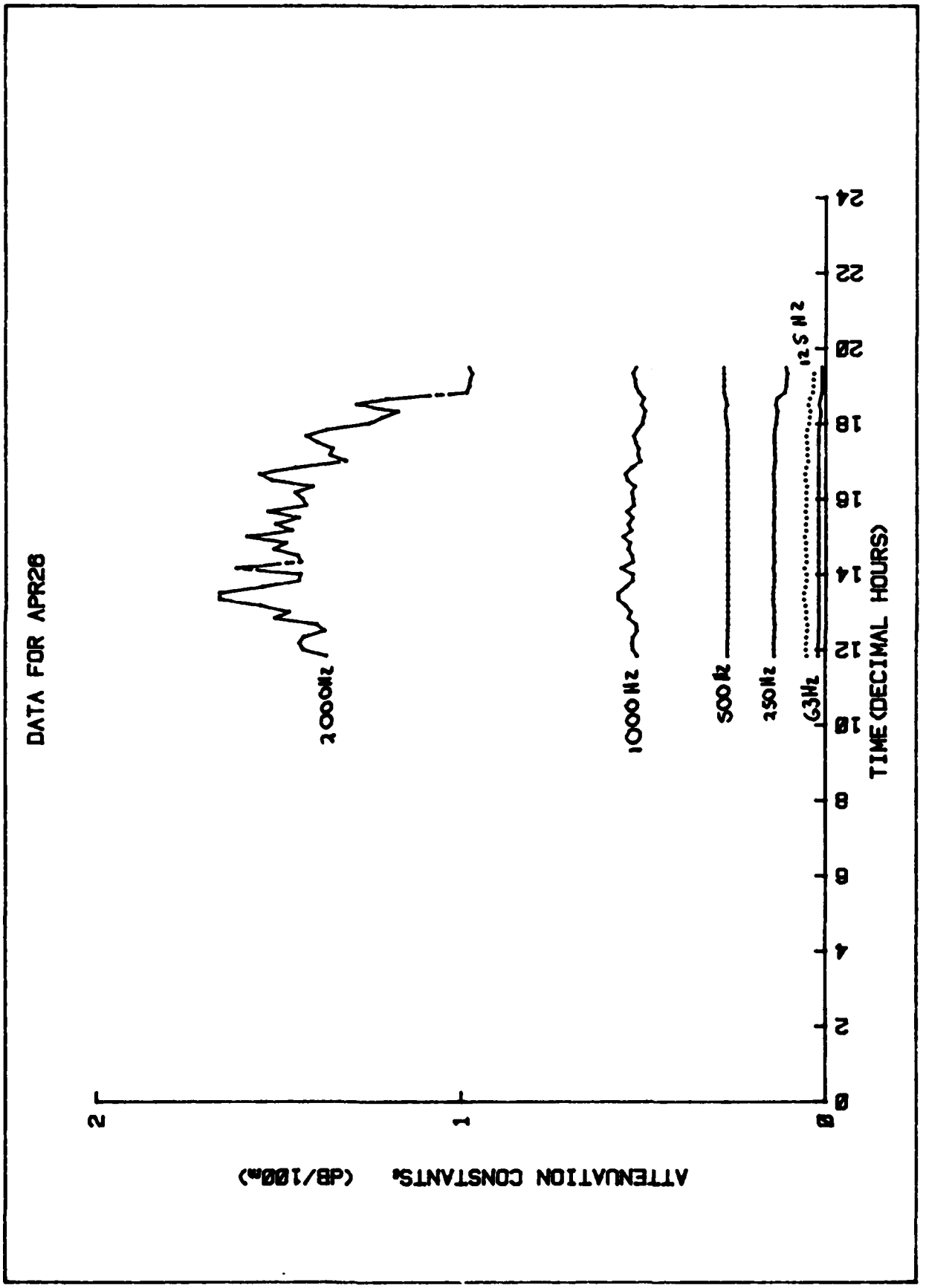

Figure 4c: Octave band attenuation constants at frequencies ranging from 63 to 2000 Hz

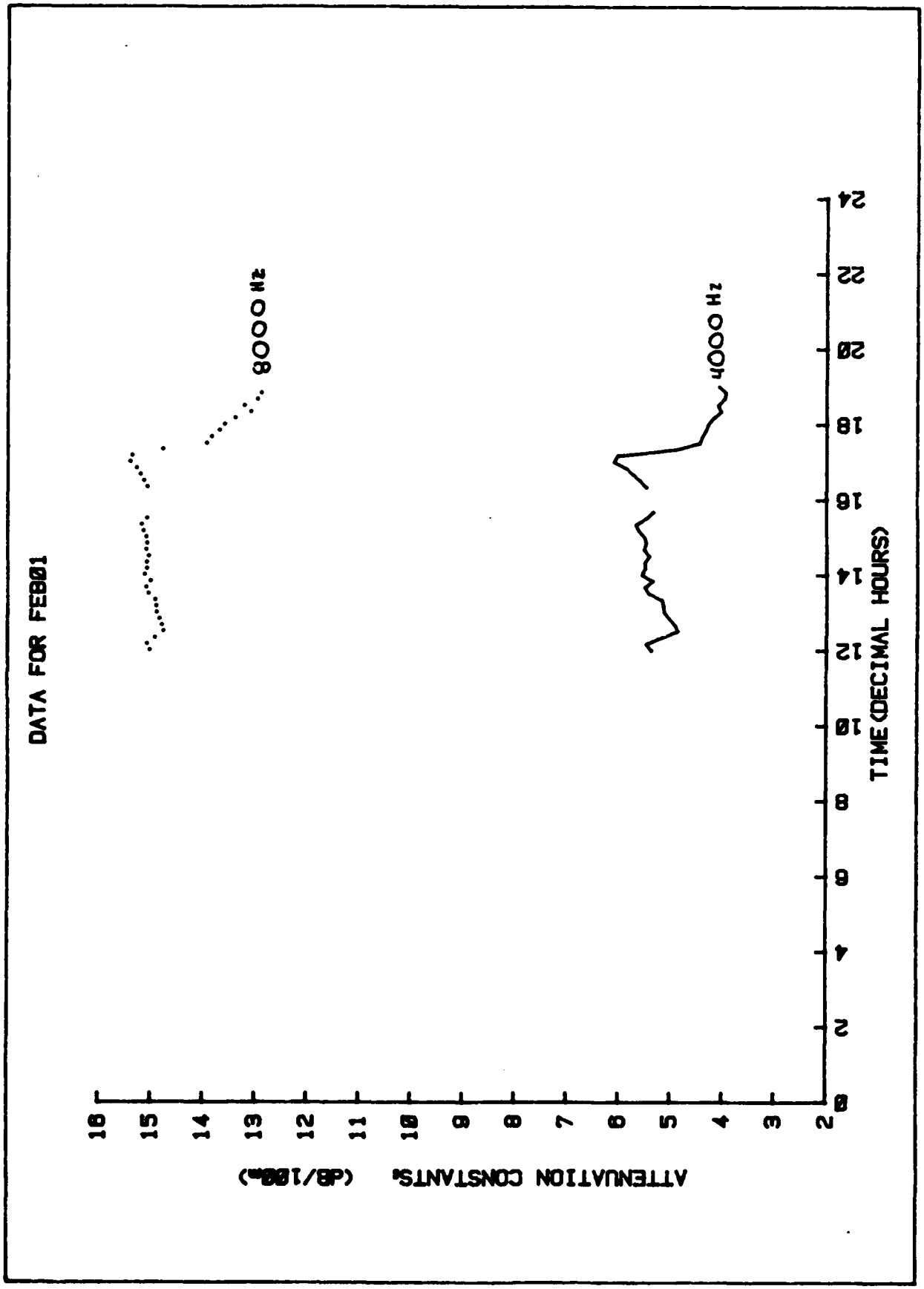

Figure 5a: Attenuation constants for 4000 and 8000 Hz for 1 February 1984.

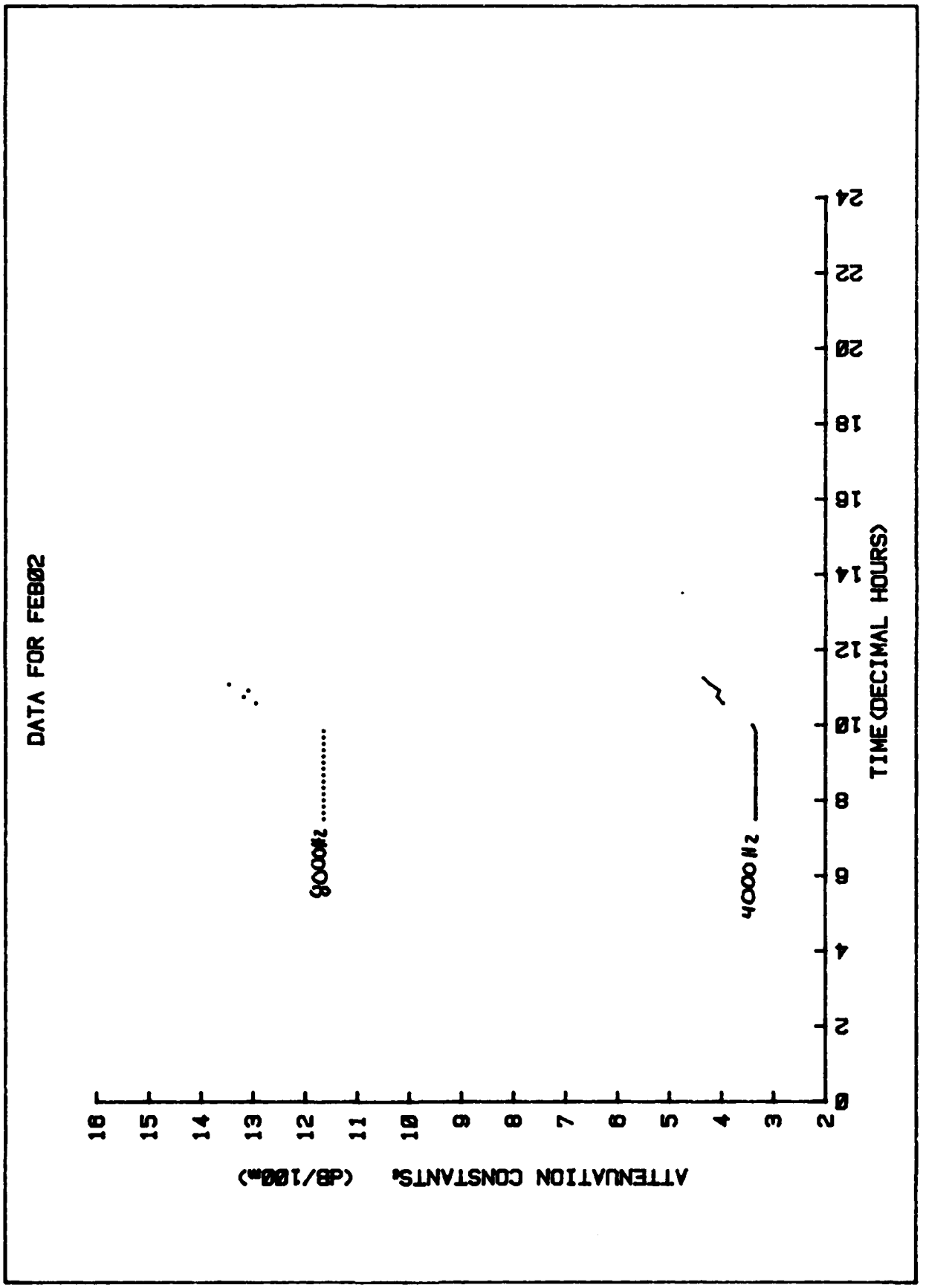

Figure 5b. Attenuation constants for 4000 and 8000 Hz for 2 February 1984

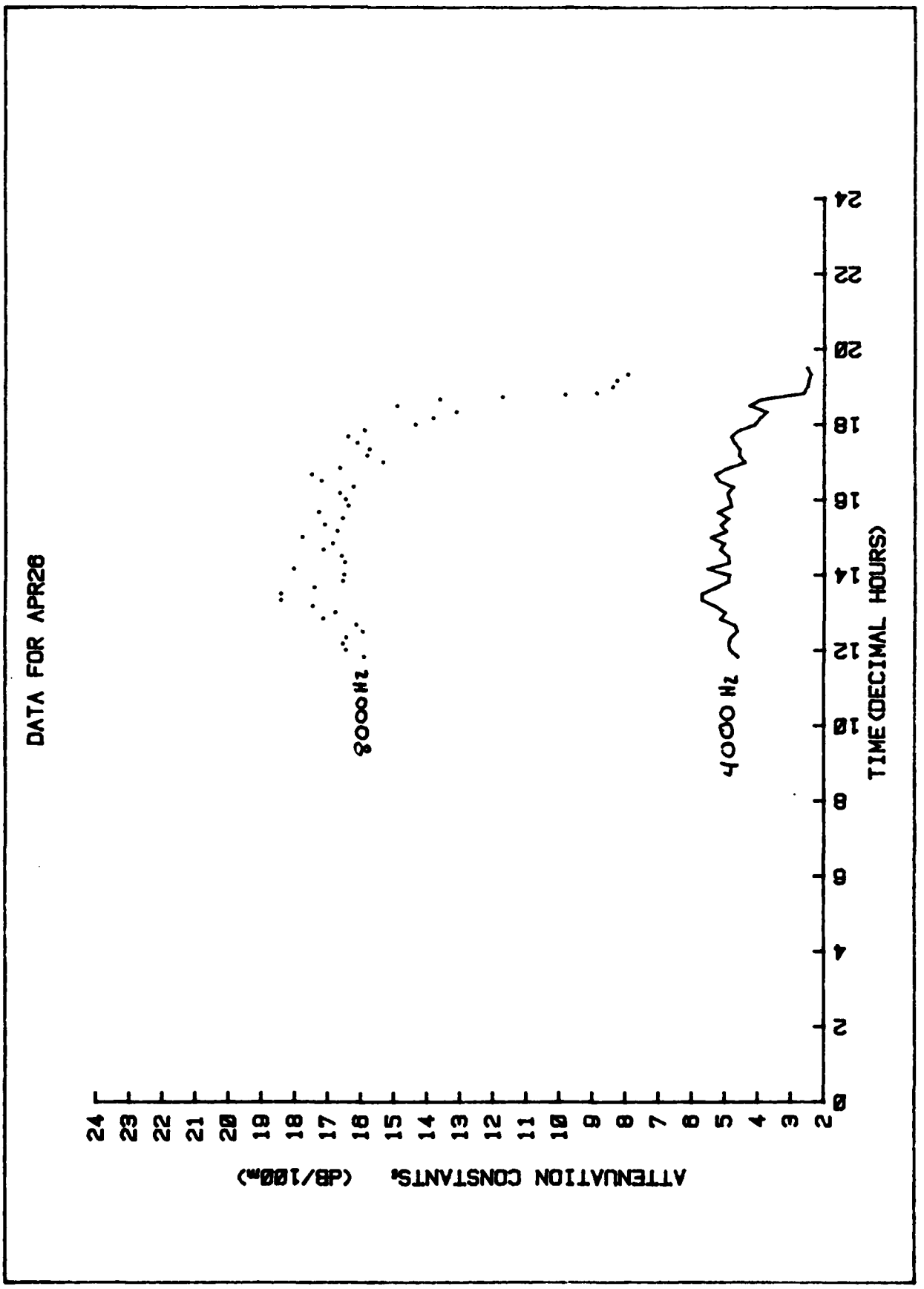

Figure 5c: Attenuation constants for 4000 and 8000 Hz for 26 April 80A

over an extended path, could be attributed to temporal variability of the relative humidity. Since the physical properties of a snow or ground surfaces also can change only slowly with respect to time, the only mechanism remaining for creating fluctuating received signals is that of relative variations in the various acoustic "rays" which make up the total received signal.

3. Description of the Multitone Acoustic Transmission and Receiving Experiment

The acoustic transmitters at approximately one-half and two meters height, simultaneously and continuously output pure tones at 24 standard 1/3 octave center frequencies from 40 to 8000 Hz, 12 frequencies at each source height. Laboratory microphones are situated at one-half and two m height at 30, 60 and 120 m from the sources. Geophones were also installed at 60 and 120 m, buried just below the ground surface. The pure tone signals are split between the two speakers as indicated in Table 1.

In this way, we can simultaneously observe propagation phenomena at two source heights and still have a reasonable number of data points to observe frequency dependence. The acoustic data acquisition system is shown in Figure 6.

Table 1. Summary of Transmitter Height and Frequencies

Transmitter A (≃ 0.5m)	Transmitter B (≃ 2 m)
40	50
63	80
100	125
160	200
250	315
400	500
630	800
1000	1250
1600	2000
2500	3150
4000	5000
6300	800

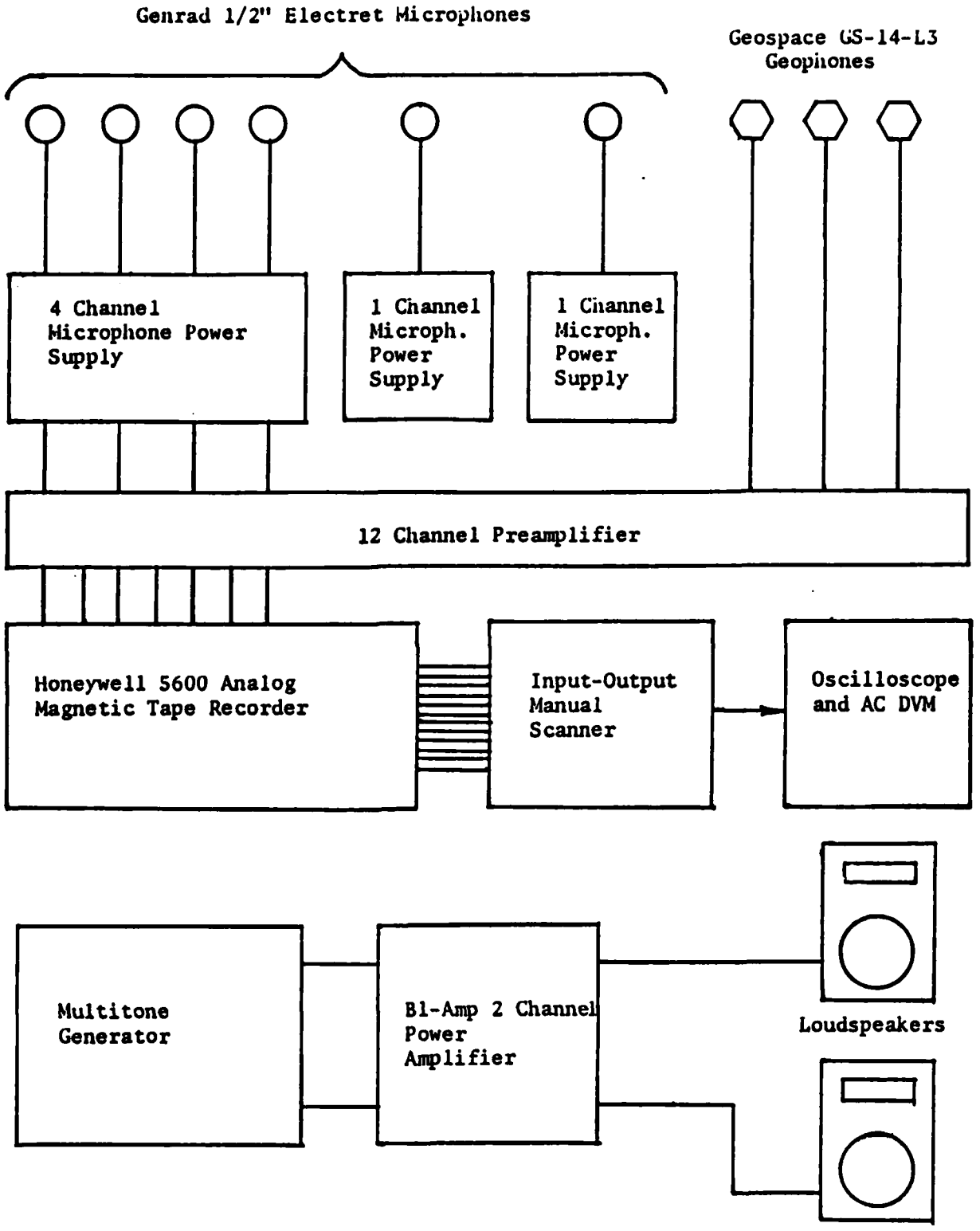

Figure 6: Data Acquisition System

4. Summary of the Acoustic Signal Data Processing

a. Preliminary Time History Analysis

Preliminary analysis of 15 minute samples of some typical time histories are shown in Figures 8 through 19 for the winter and spring experiments. Using the setup shown in Figure 7, the winter and spring samples start at 11:54 a.m. and 1:56 p.m., respectively. All microphone heights are 2m. Figures 8-10 show overall levels (all 1/3 octave filters summed) for the 30, 60 and 120m source to receiver distance (range). The fluctuations are reasonably small with slightly lower average levels for the spring observations. There is a general trend of large fluctuations at longer range and in the spring experiment. The data have not been corrected for absolute values of microphone sensitivity and preamp gain but only differences in these values between winter and spring; therefore, comparison of averages at different ranges should not be made. In Figures 11-19 time histories are shown for 50, 500 and 5000 Hz for ranges of 30m (Figures 11-13), 60m (Figures 14-16) and 120m (Figures 17-19). It is apparent that fluctuations for individual frequencies are considerably greater than for the overall summed levels. Again, there is a general trend of greater fluctuations at higher frequencies at longer ranges, and in the spring observations. The larger fluctuations for individual frequencies indicate a strong influence of multipath enhancement and interference which is not stationary with time. The large difference in average levels between winter and spring for 500 Hz at all three ranges could be attributed to a change in ground impedance which strongly influences the frequency of the large sharp peaks in excess attenuation almost always obsrved in propagation measurements at shallow grazing angles over ground surfaces.

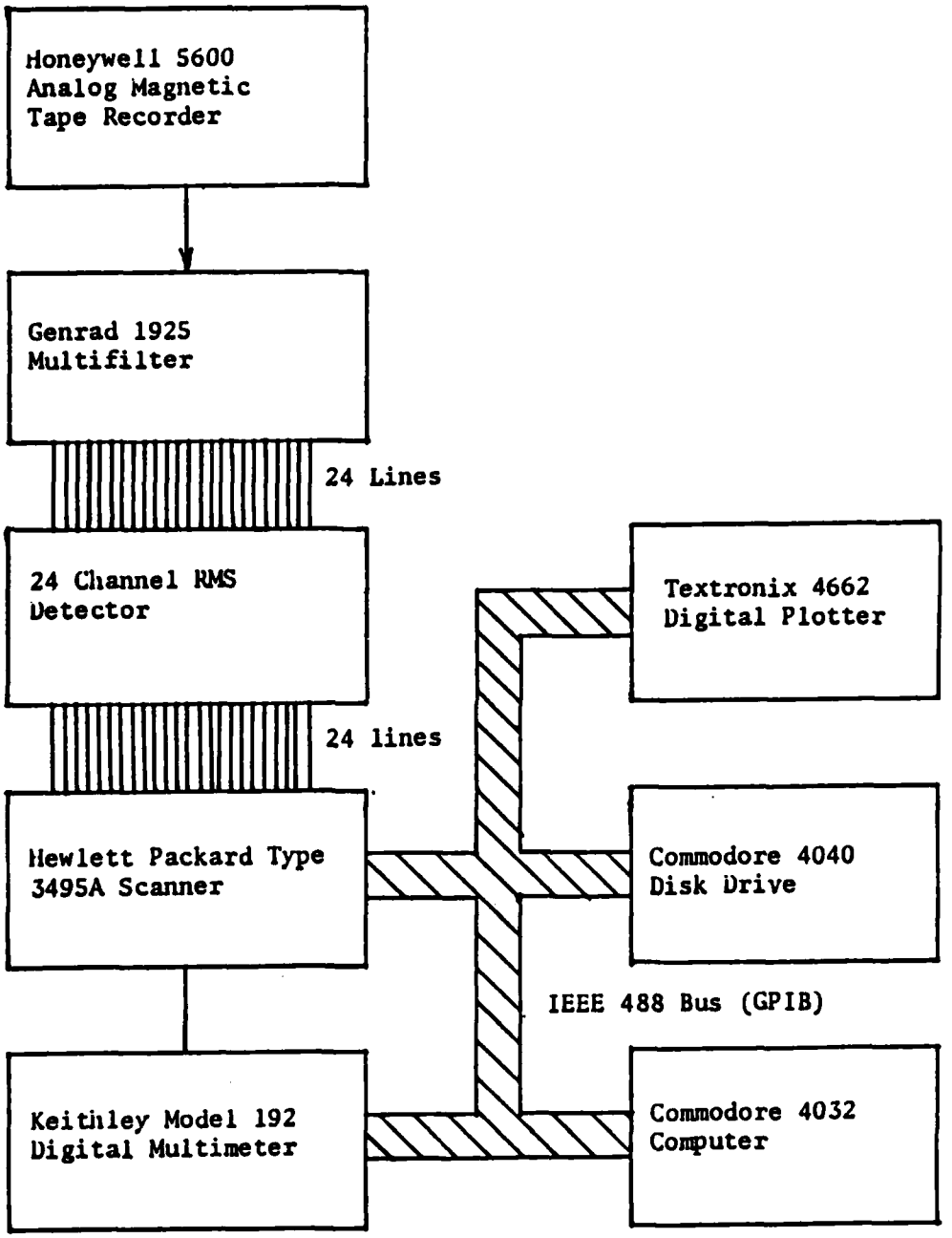

Figure 7: Data Analysis System

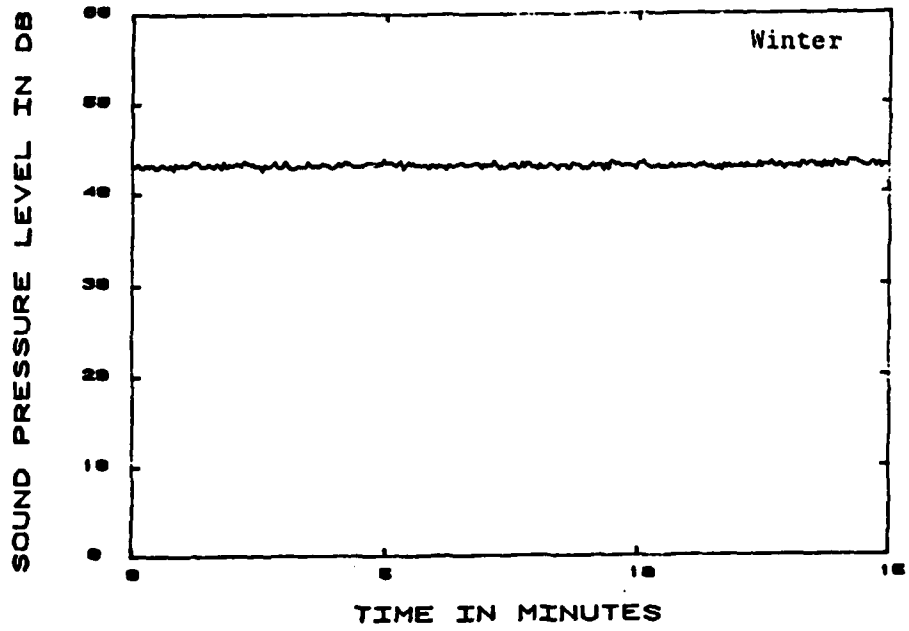

SUMMED 2M Height Microphone
Overall Level at 30M Range

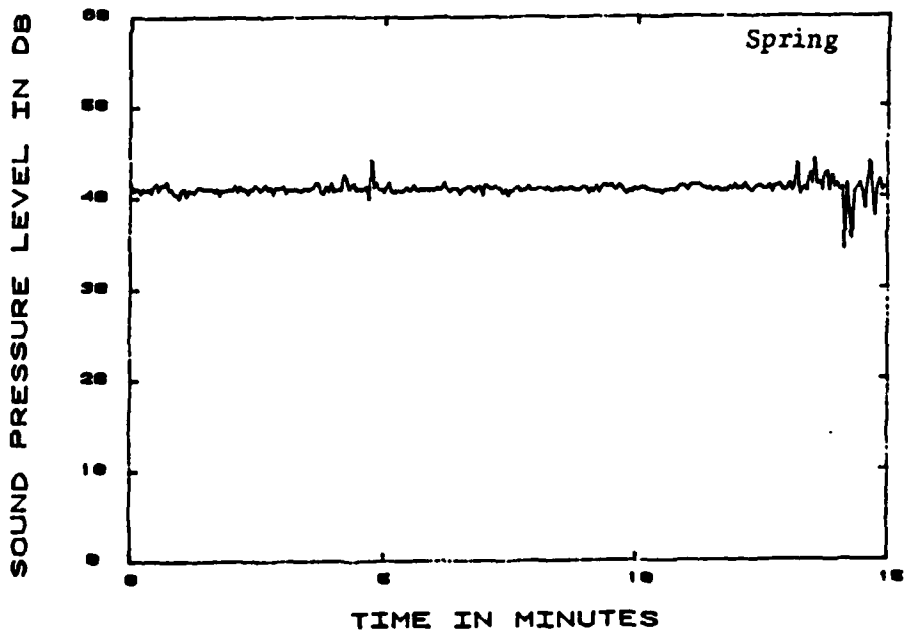

SUMMED 2M Height Microphone
Overall Level at 30M Range

Figure 8: Summed 2 Meter Height, 30 M Range

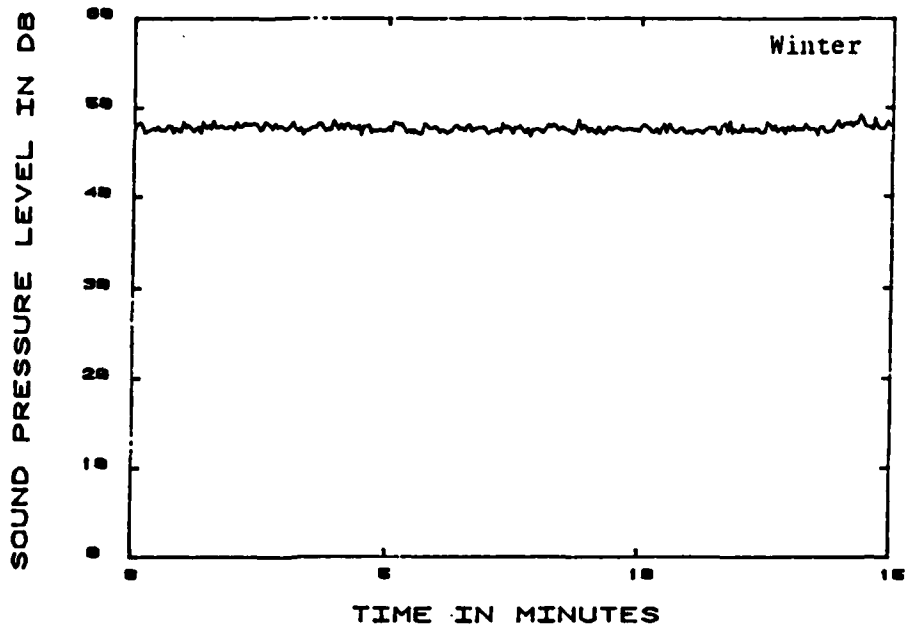

SUMMED 2M Height Microhpone
Overall Level at 60M Range

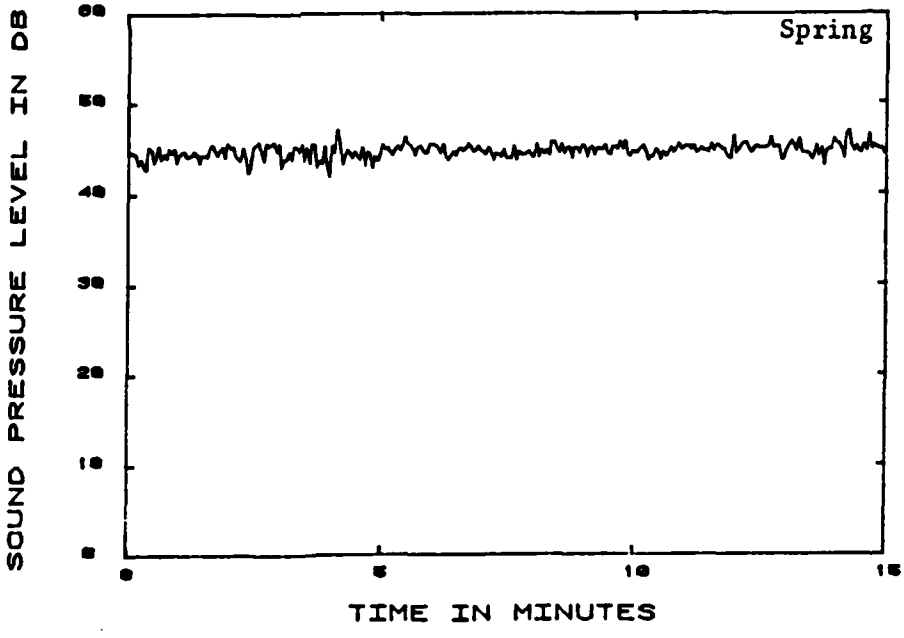

SUMMED 2M Height Microhpone
Overall Level at 60M Range

Figure 9: Summed 2 Meter Height, 60 Meter Range

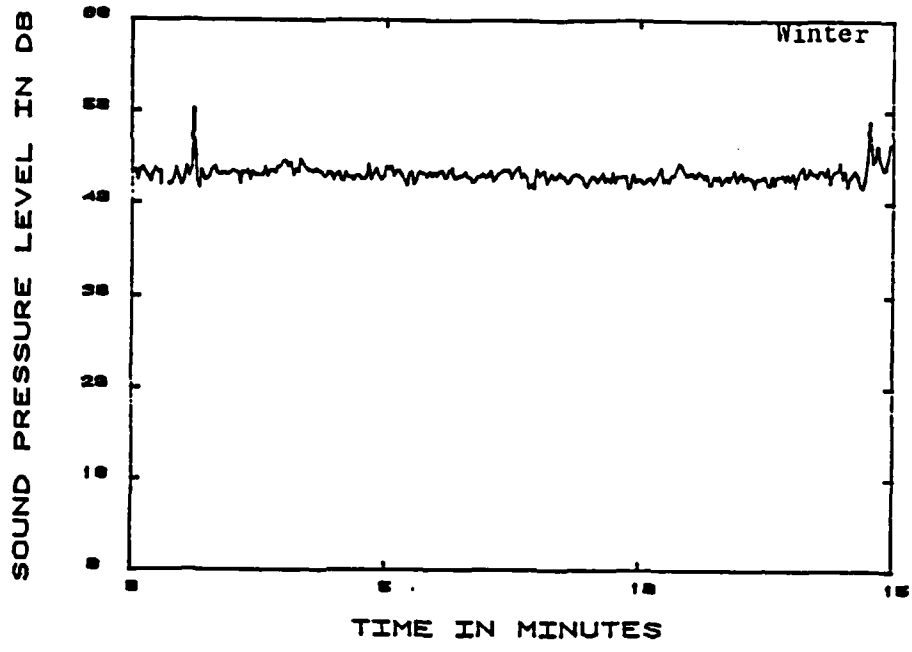

SUMMED

2M height Microphone
Overall Level at 120 M Range

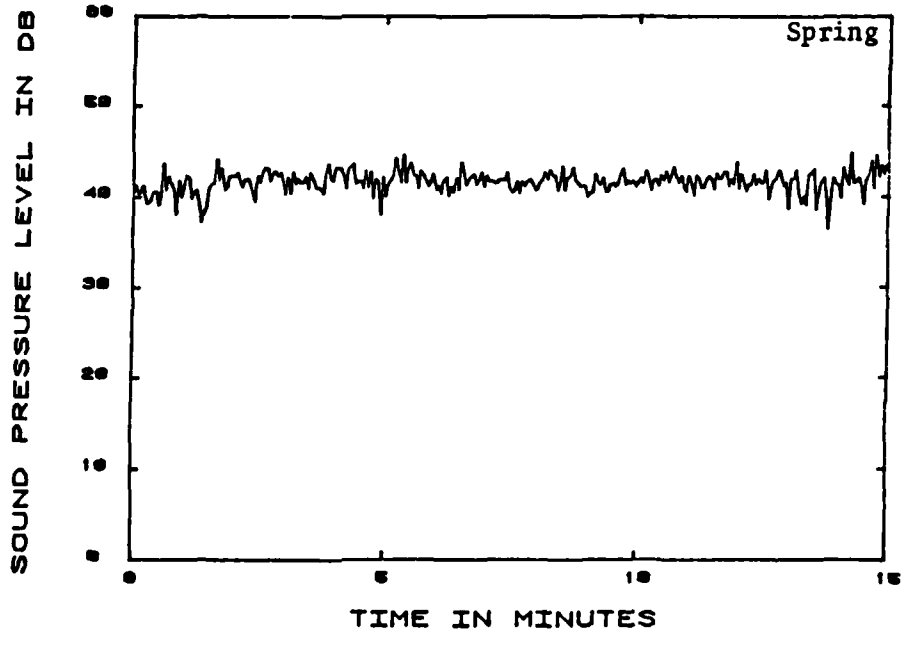

SUMMED

2M Height Microphone
Overall Level at 120M Range

Figure 10: Summed 2 Meter Height, 120 Meter Range

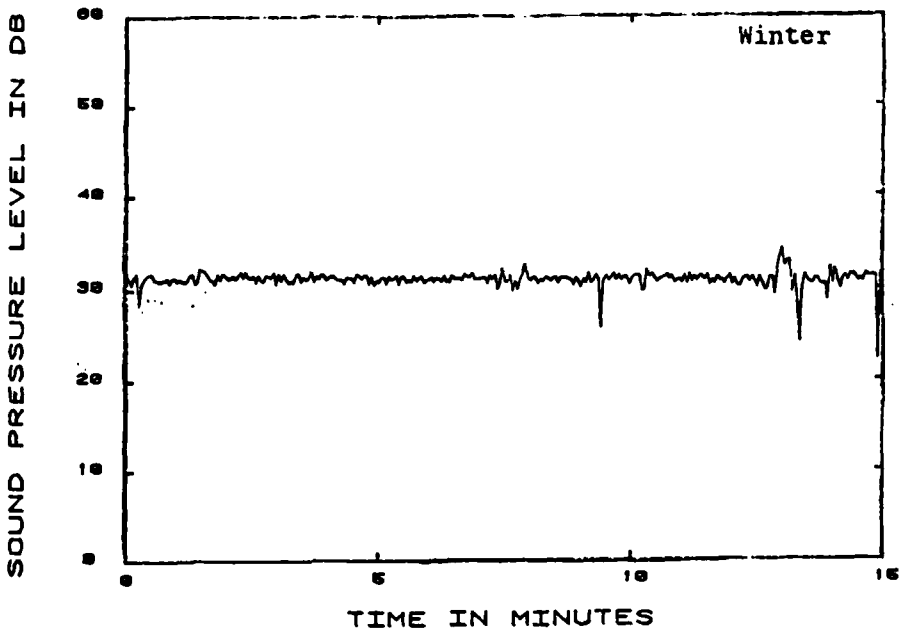

50 HZ

2M Height Microhpone
50 Hz Level at 30M Range

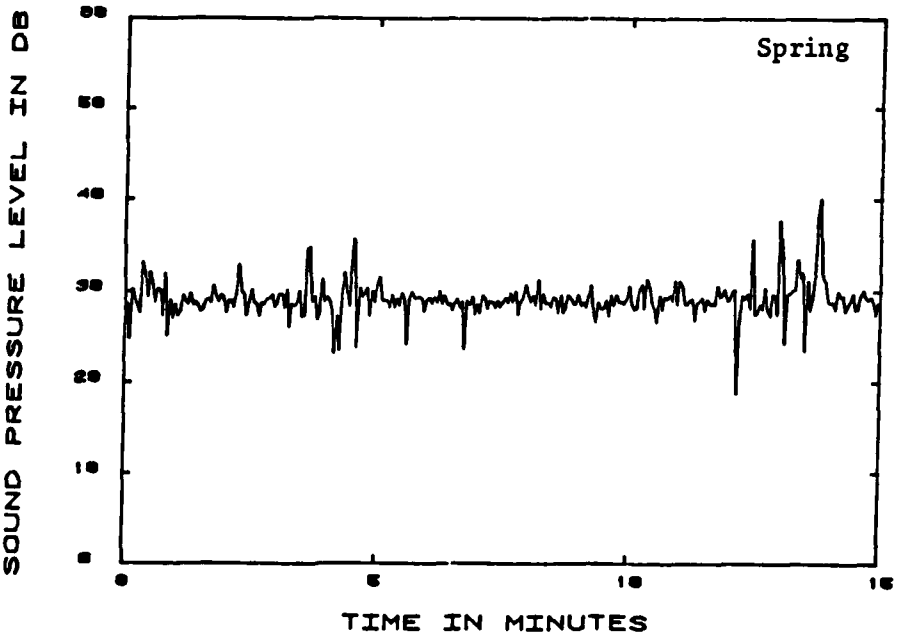

50 HZ

2M Height Microphone
50 Hz Level at 30M Range

Figure 11: 50 Hz 2 Meter Height, 30 Meter Range

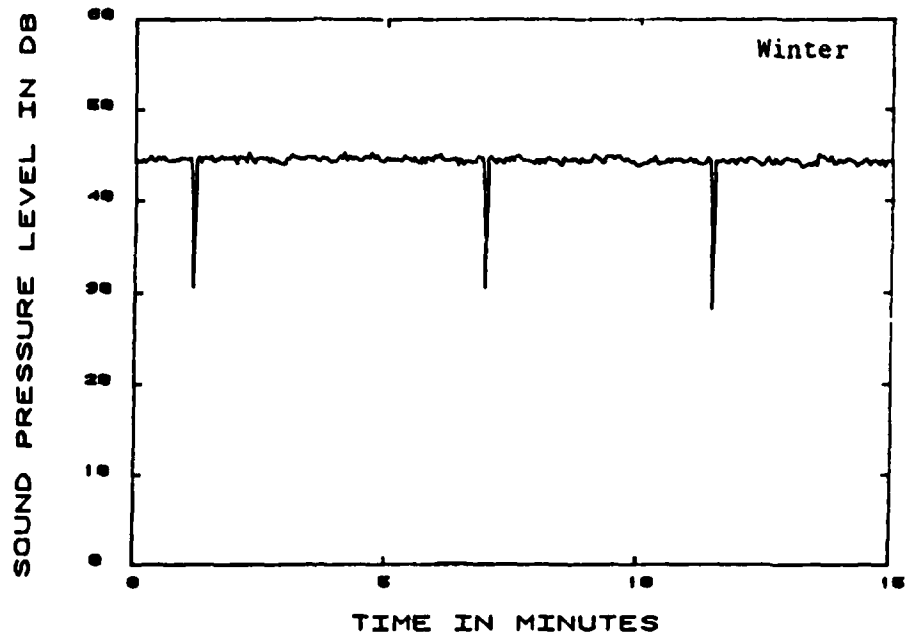

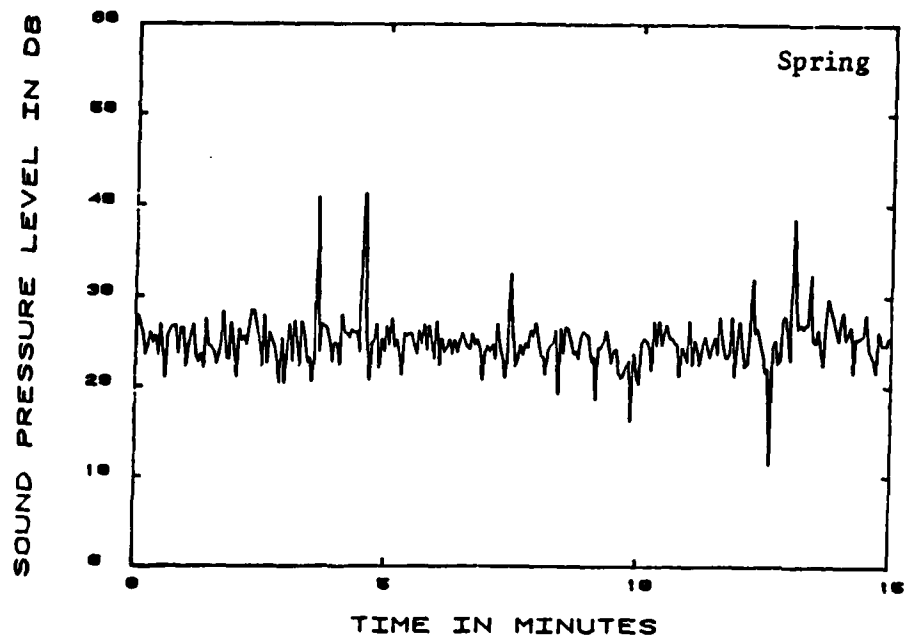

Figure 12: 500 Hz 2 Meter Height, 30 Meter Range

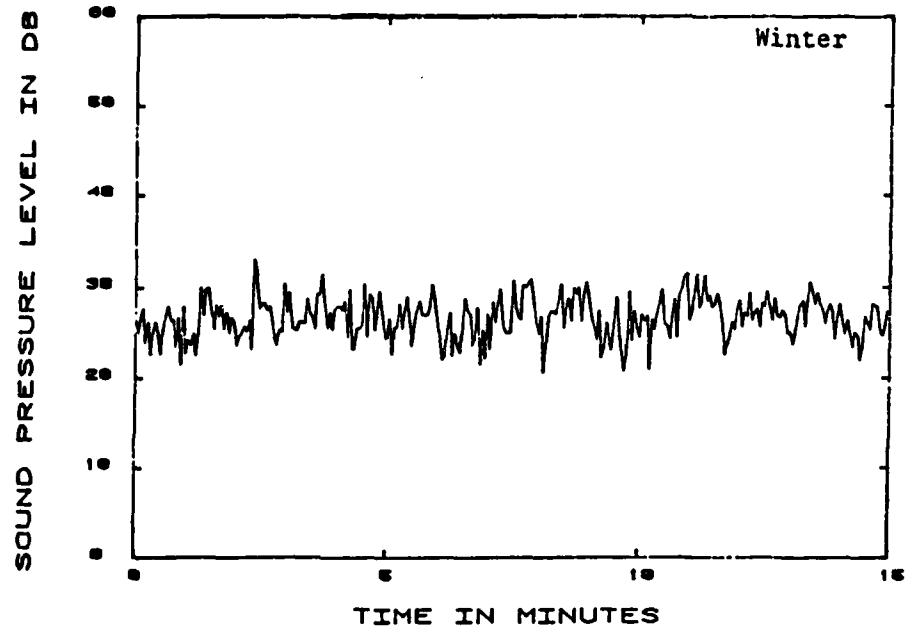

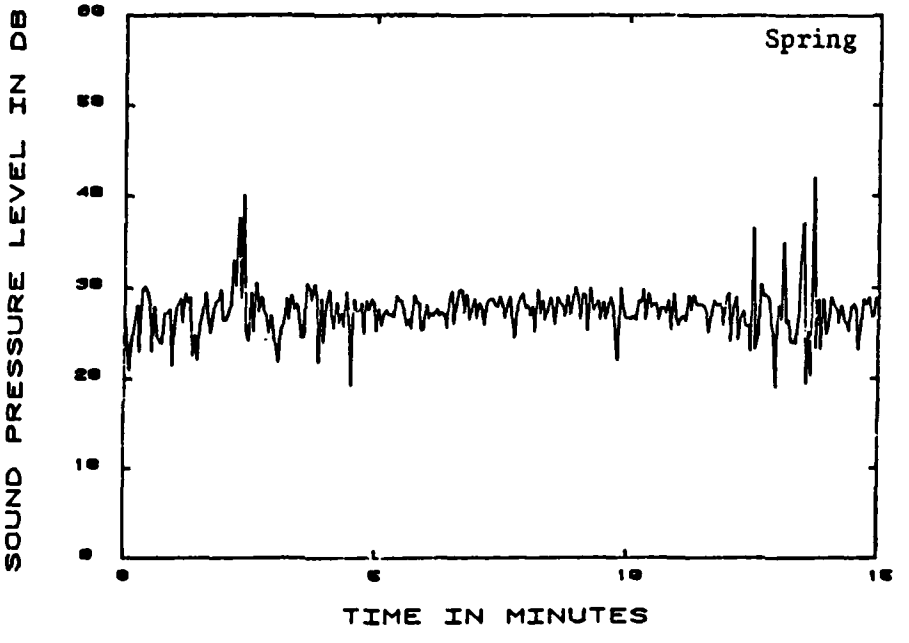

Figure 13: 5k Hz 2 Meter Height, 30 Meter Range

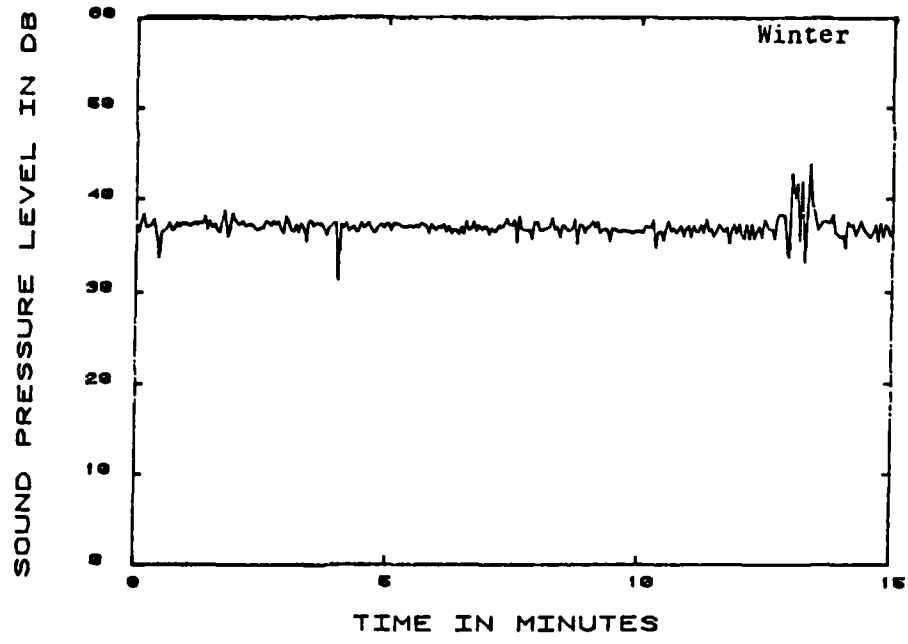

50 HZ

2M Height Microphone
50 Hz at 60M Range

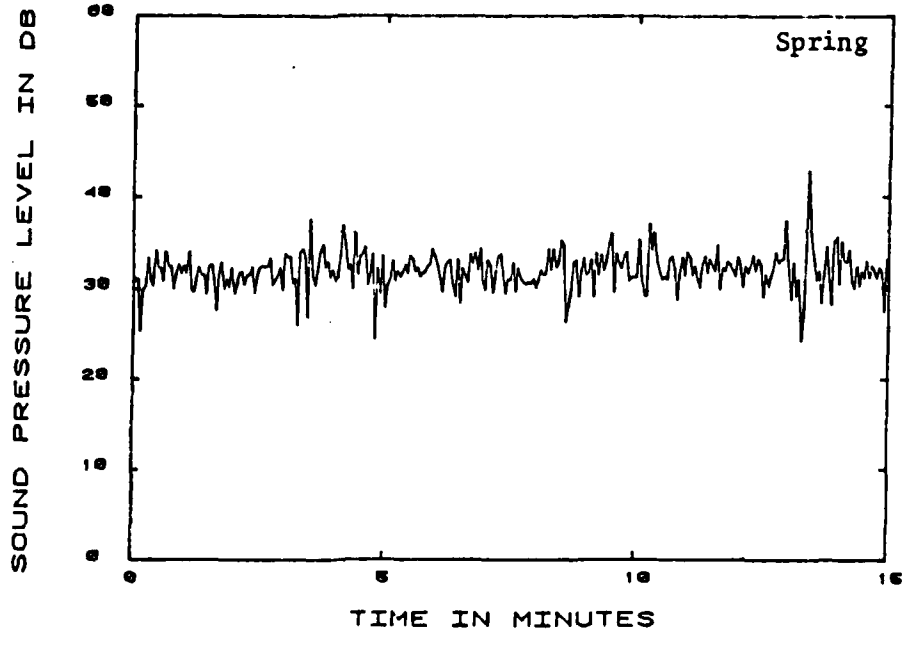

50 HZ

2M Height Microphone
50 Hz at 60M Range

Figure 14: 50 Hz 2 Meter Height, 60 Meter Range

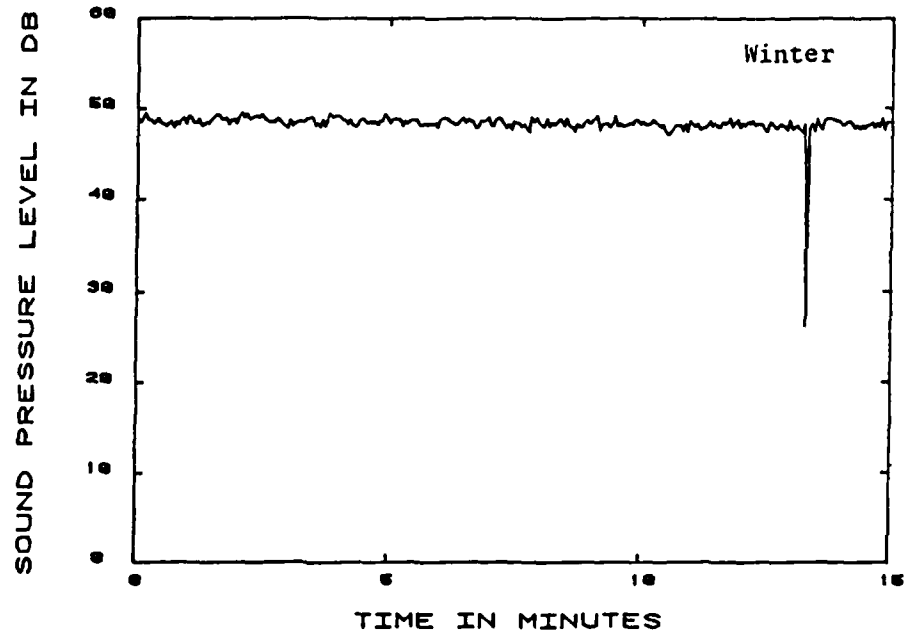

500 HZ

2M Height Microhpone
500 Hz Level at 60M

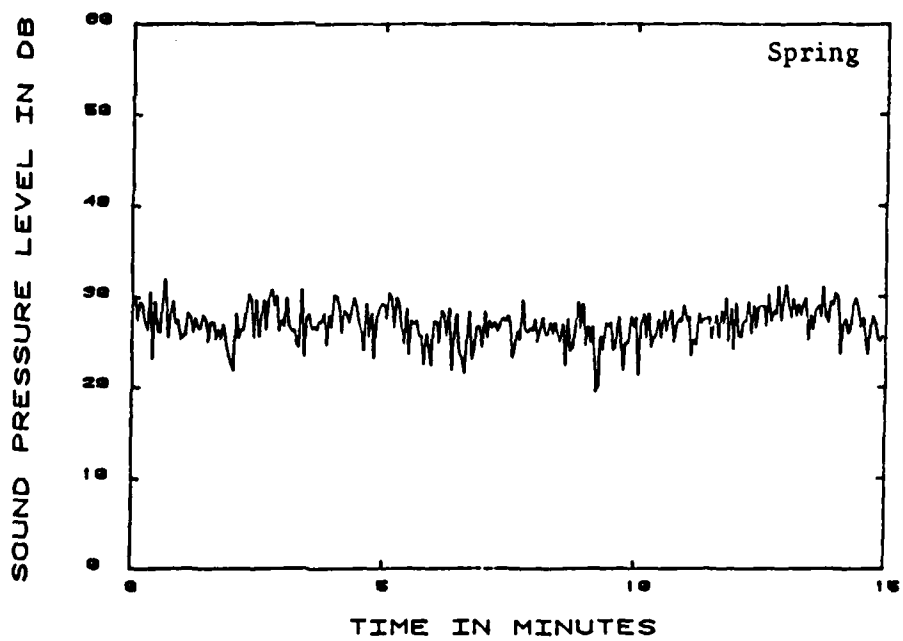

500 HZ

2M Height Microphone
500 Hz Level at 60M

Figure 15: 500 Hz 2 Meter Height, 60 Meter Range

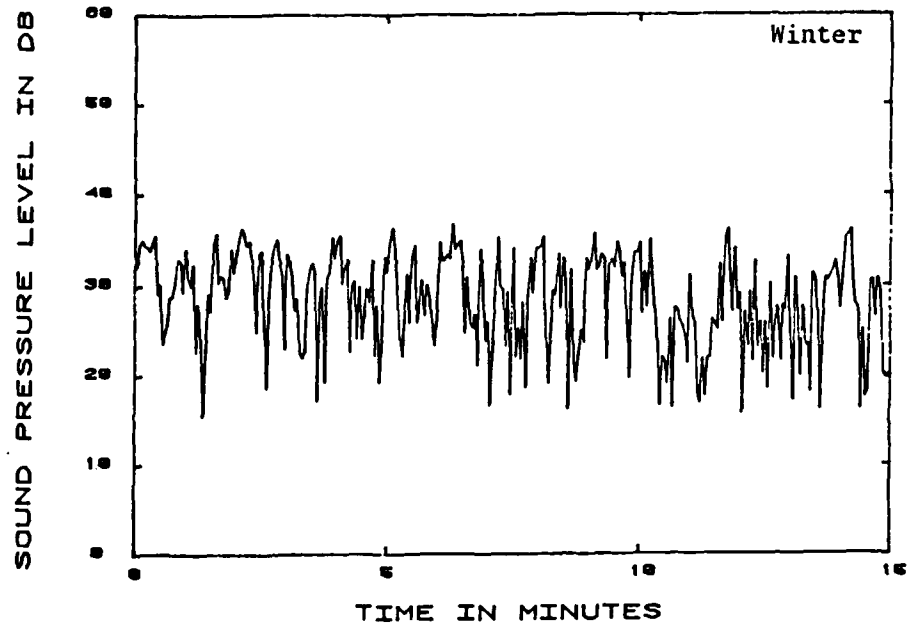

5K HZ

2M Height Microphone
5000 Hz Level at 60M Range

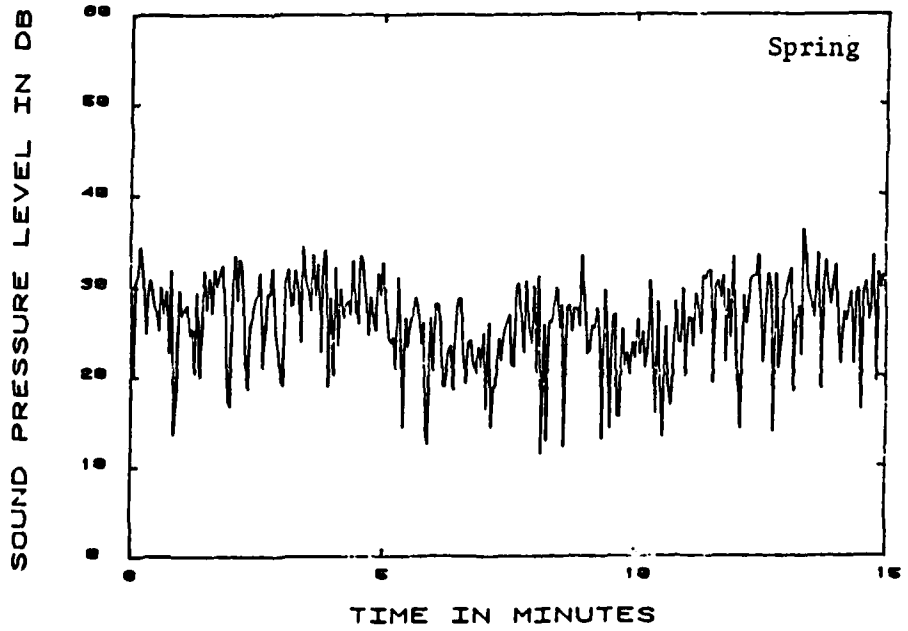

5K HZ

2M Height Microphone
5000 Hz Level at 60M Range

Figure 16: 5 Hz 2 Meter Height, 60 Meter Range

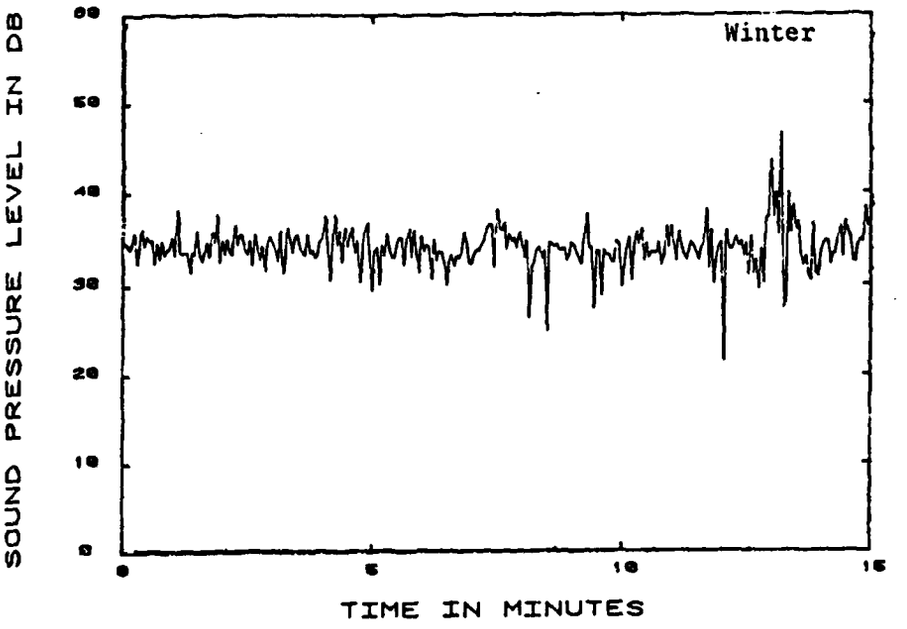

50 HZ

2M Height Microphone
50 Hz Level at 120M Range

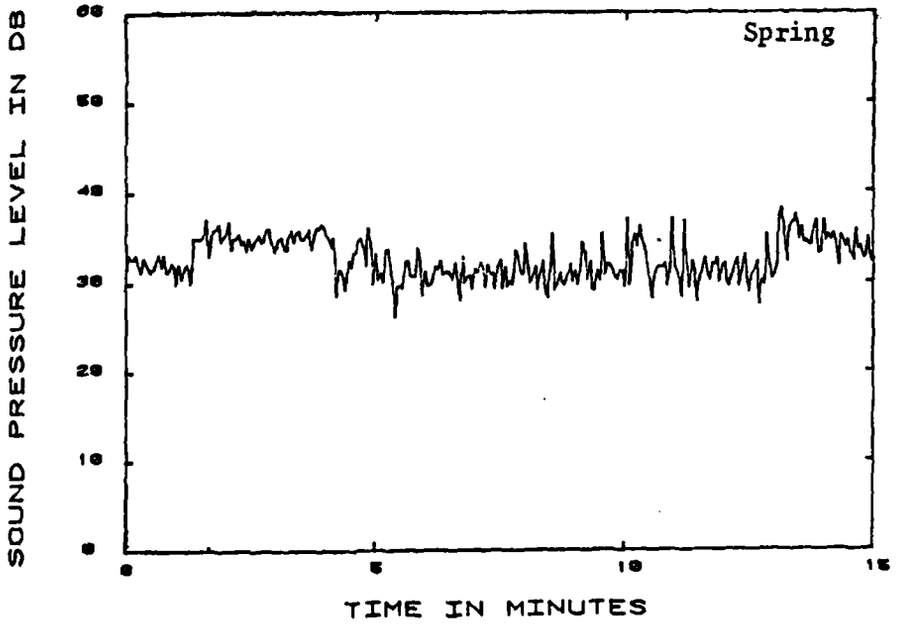

50 HZ

2M Height Microphone
50 Hz Level at 120M Range

Figure 17: 50 Hz 2 Meter Height, 120 Meter Range

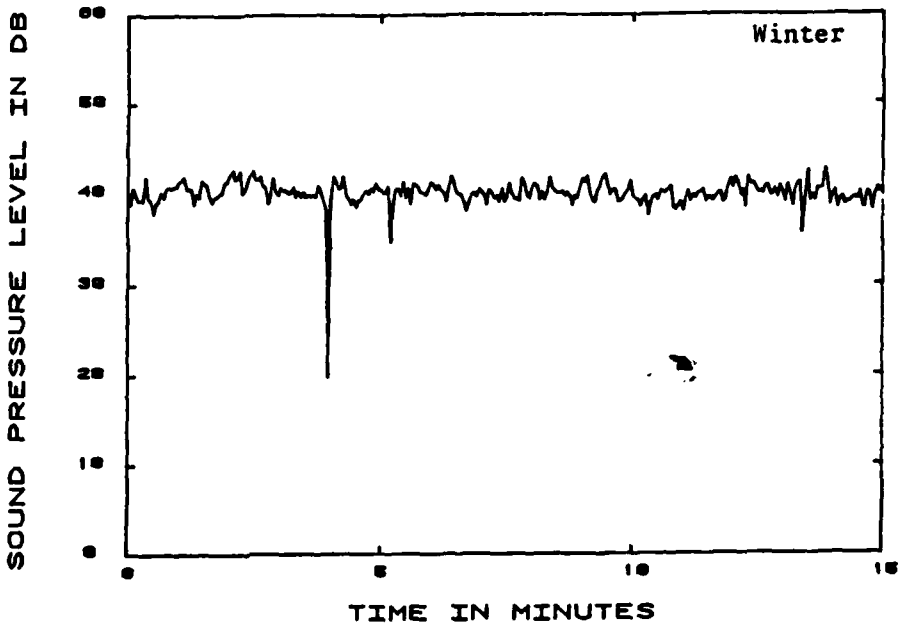

500 HZ

2M Height Microphone
500 Hz Level at 120M Range

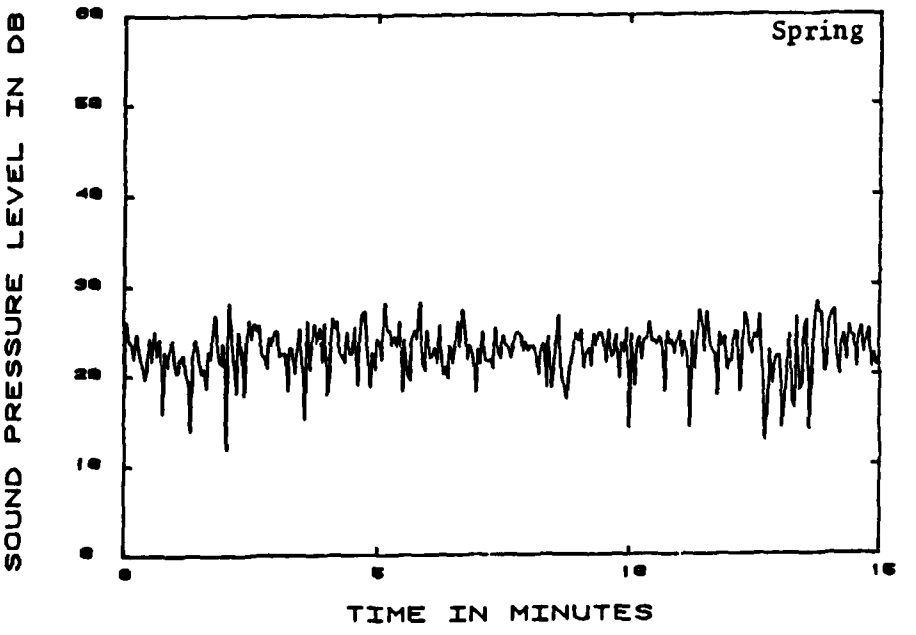

500 HZ

2M Height Microphone
500 Hz Level at 120M Range

Figure 18: 500 Hz 2 Meter Height, 120 Meter Range

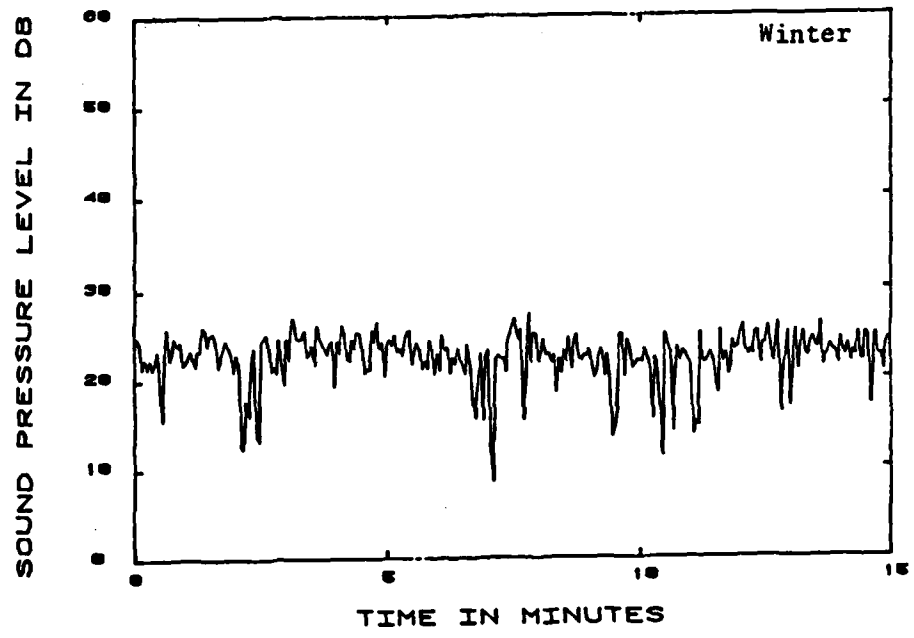

5K HZ

2M Height Microphone
5000 Hz Level at 120M Range

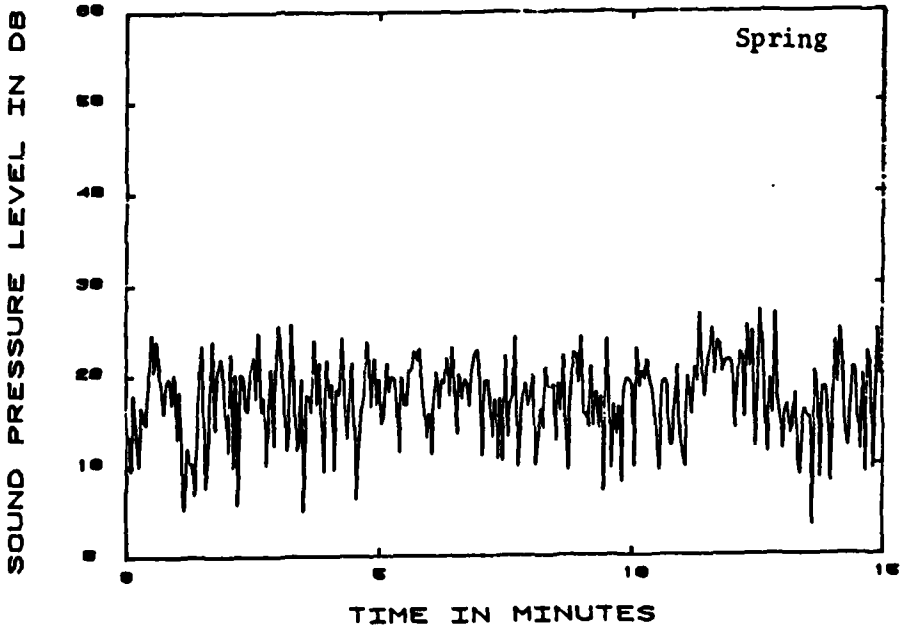

5K HZ

2M Height Microphone
5000 Hz Level at 120M Range

Figure 19: 5k Hz 2 Meter Height, 120 Meter Range

b. Statistical Analysis for Comparison with Meteorological Data

For this task the time periods stated in section 1 (13:55-L4118 on 1 Feb. and 13:56-14:19 on Apr 26) were chosen to obtain cumulative probability distributions. The Tape Recorder, Multifilter and 24 Channel RMS Detector shown in figure 7 were used in conjunction with a high-speed multiplexer A/D converter and an IBM PC to digitize the data and store it on disk. Software was then written to obtain the cumulative probability distribution of the peak amplitude of the sound pressure levels in dB re $2x10^{-5}$ pascals. The data ar plotted in terms of dB about the mean level on the x axis versus a scale on the y axis where

$$g(y) = \int_0^y y \exp\left(-y^2/2\right)$$

and g(y) is the probability of the amplitude being below the level x - (RMS SOUND PRESSURE LEVEL). This is equivalent to plotting the data on Rayleigh probability graph paper.

The statistical data are shown in figures 20 through 34. The lower grequency in each graph is denoted by the square symbol and the root mean square average sound pressure level for each sample period os denoted at the bottom of each graph.

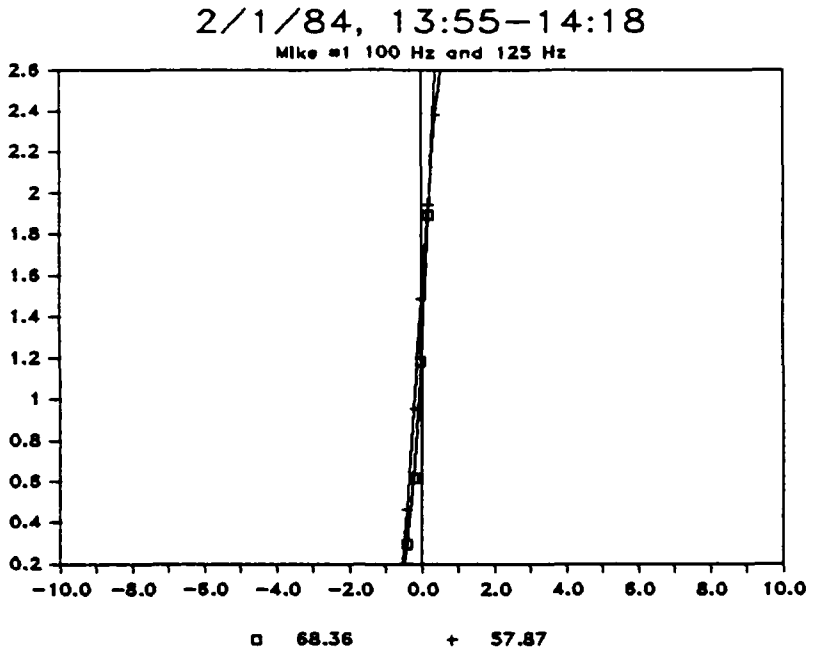

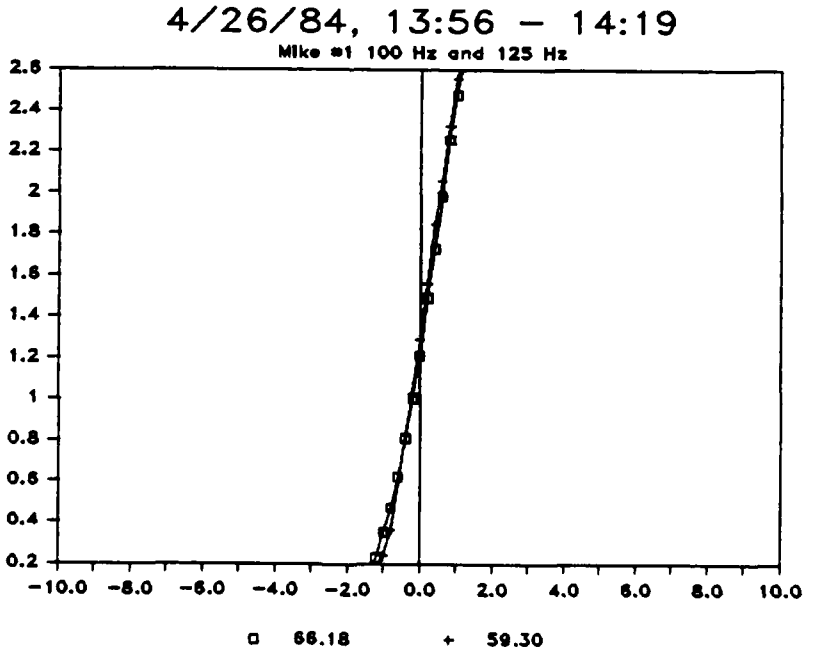

Figure 20: 2 Meter Height, 30 Meter Range

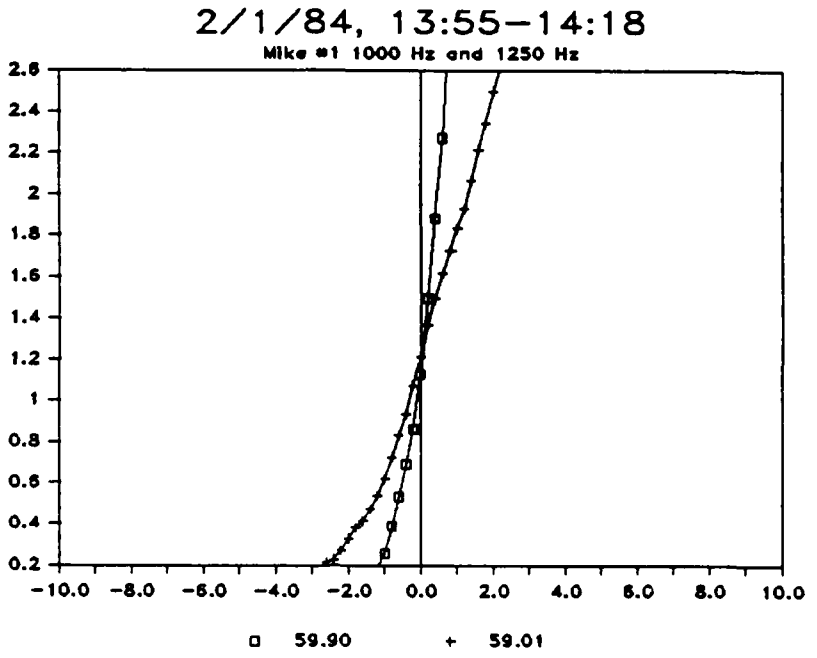

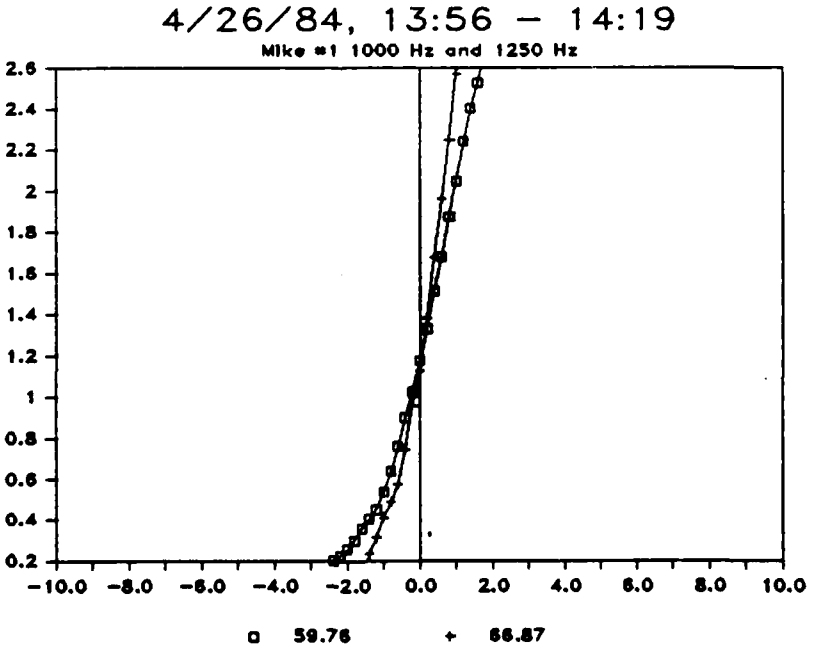

Figure 21: 2 Meter Height, 30 Meter Range

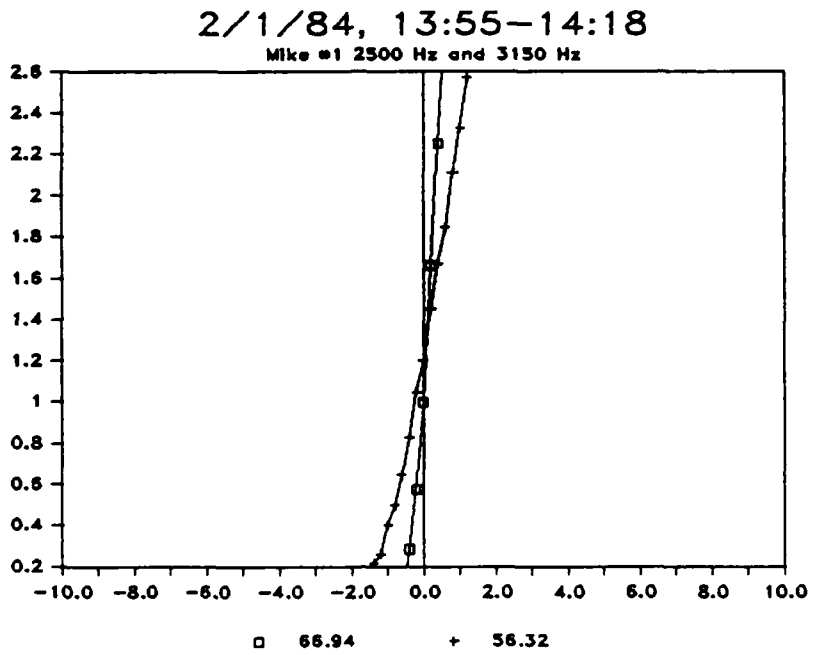

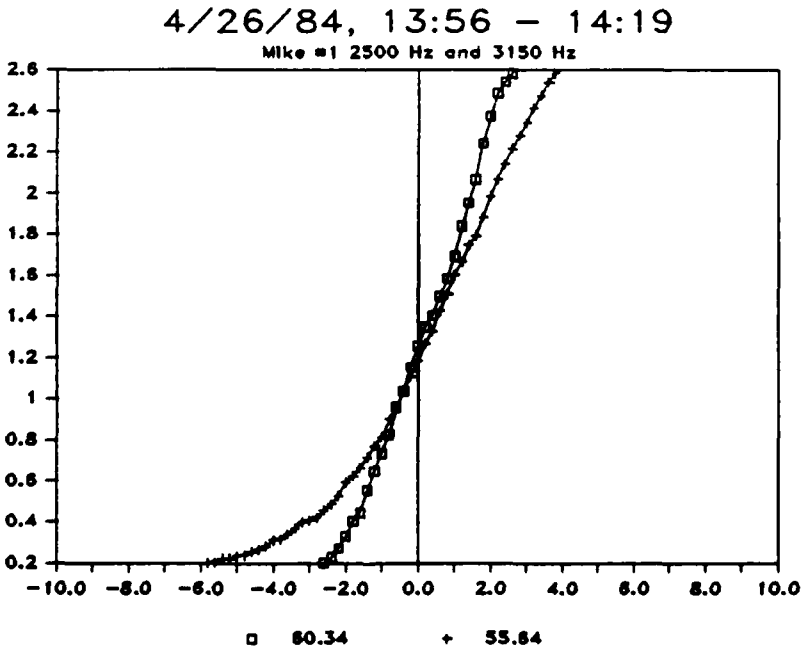

Figure 22: 2 Meter Height, 30 Meter Range

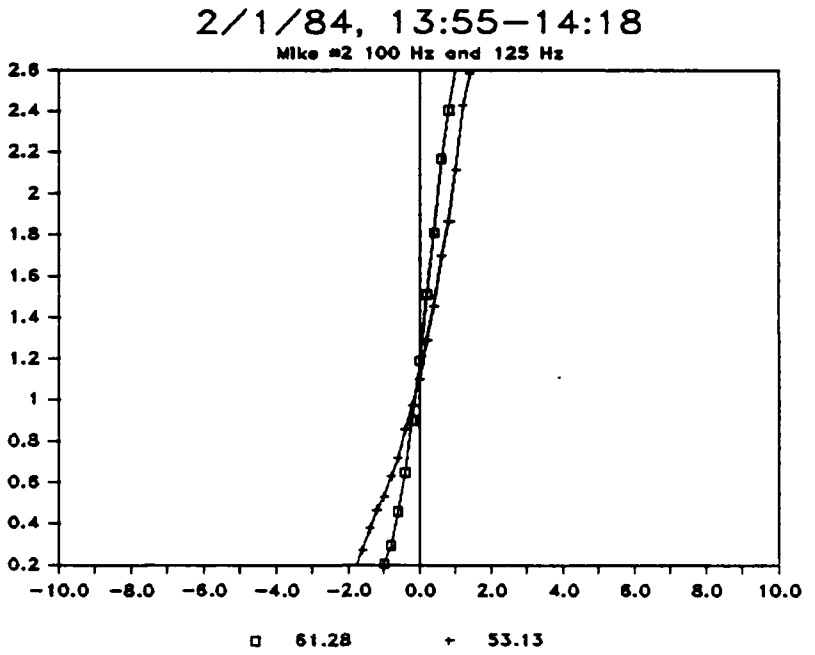

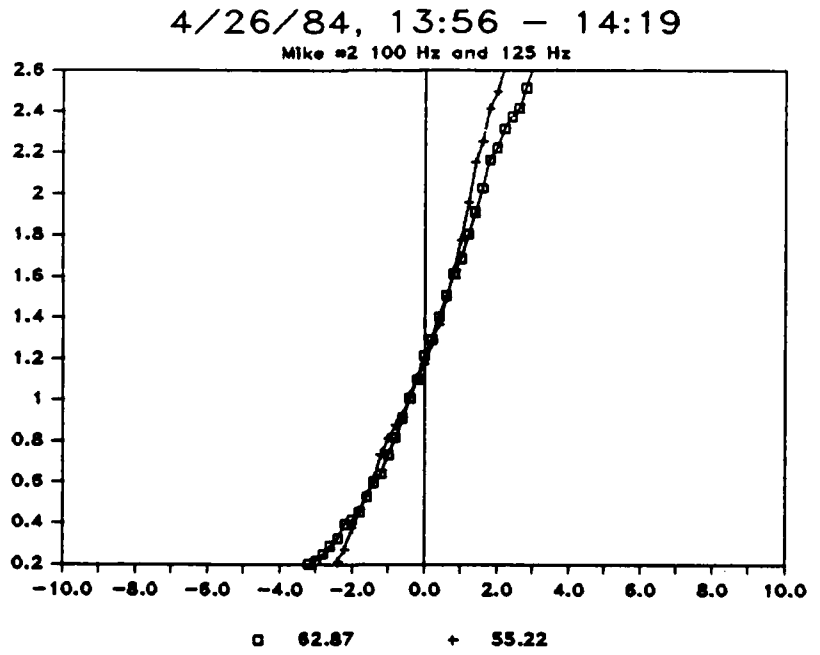

Figure 23: .5 Meter Height, 60 Meter Range

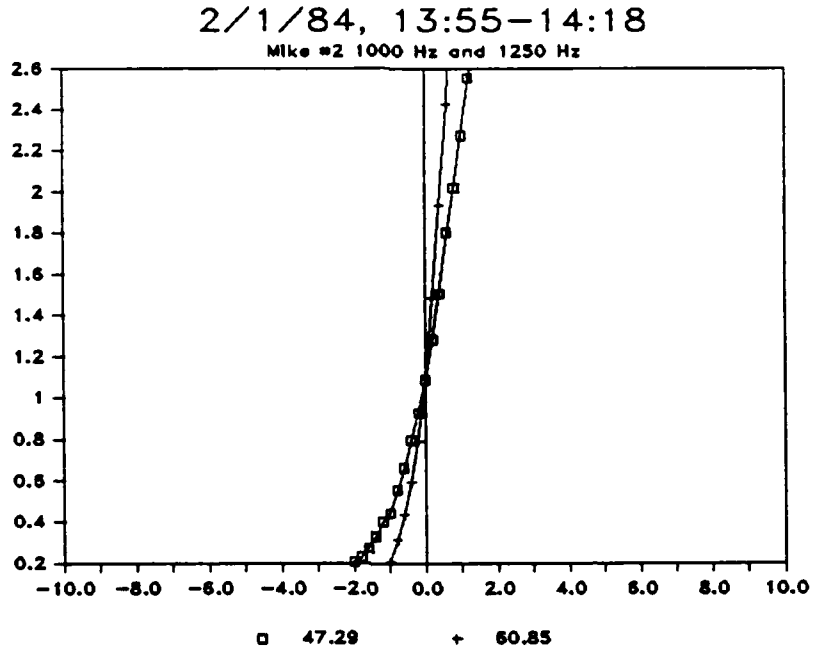

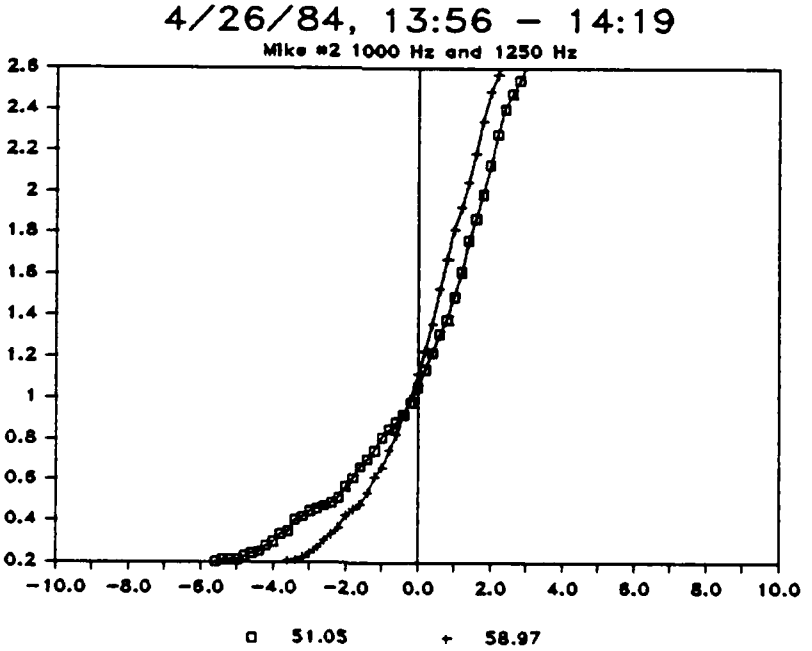

Figure 24: ,5 Meter Height, 60 Meter Range

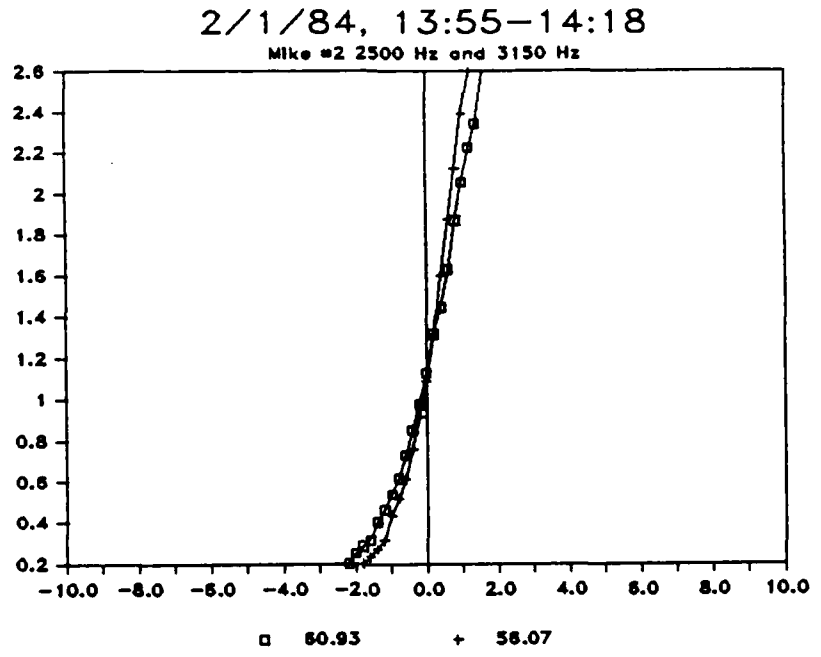

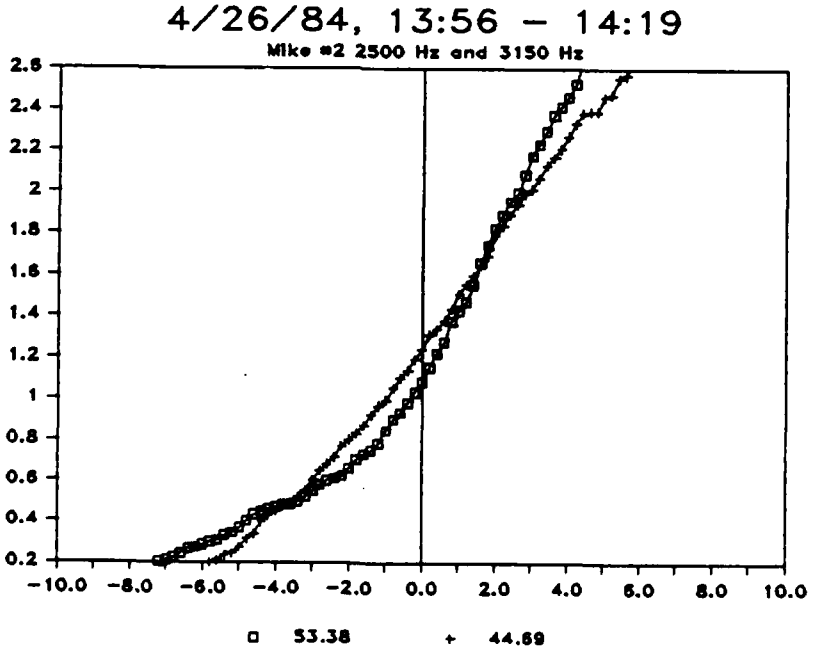

Figure 25: .5 Meter Height, 60 Meter Range

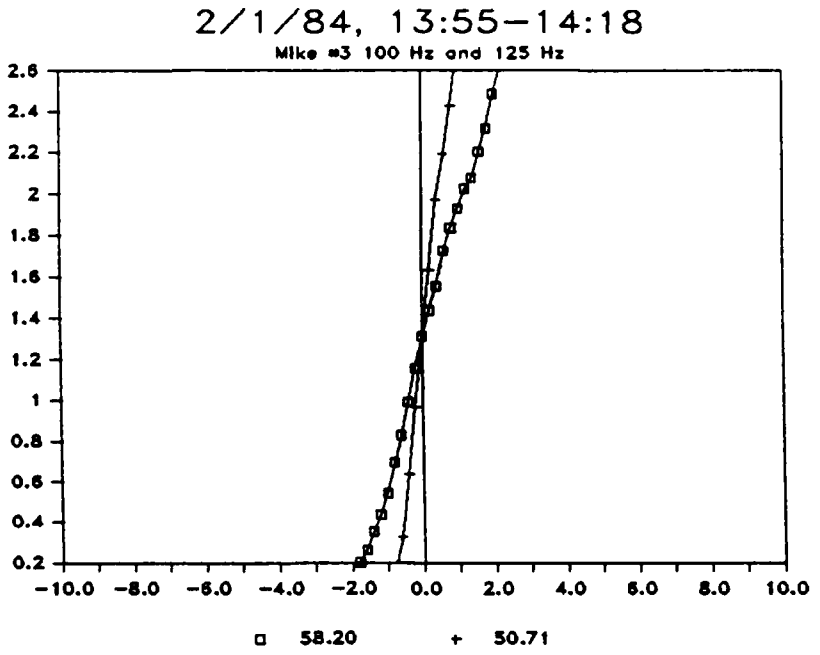

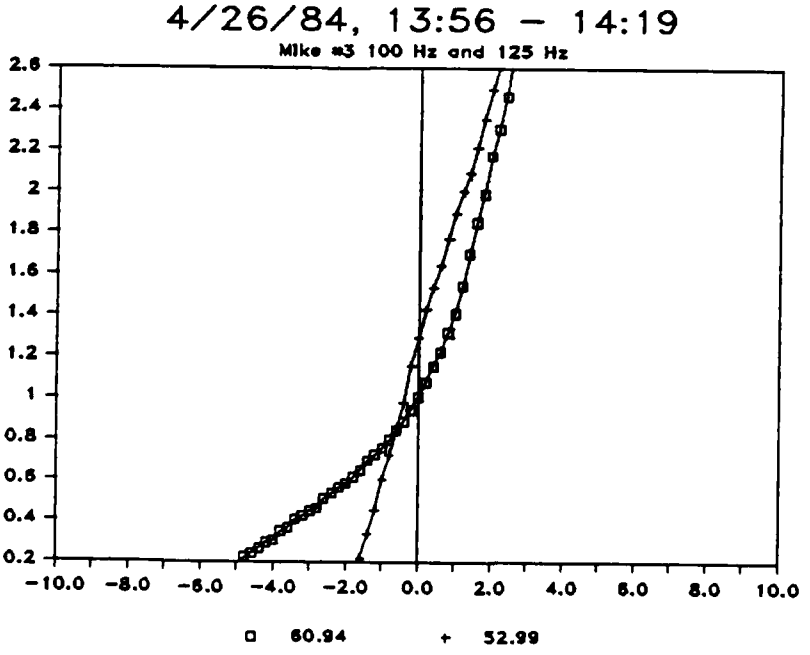

Figure 26: 2 Meter Height, 60 Meter Range

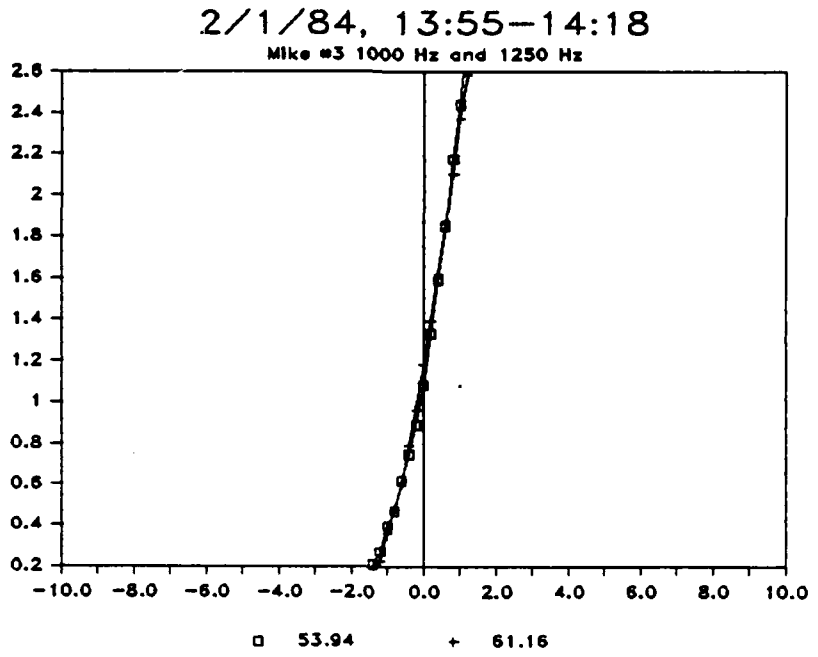

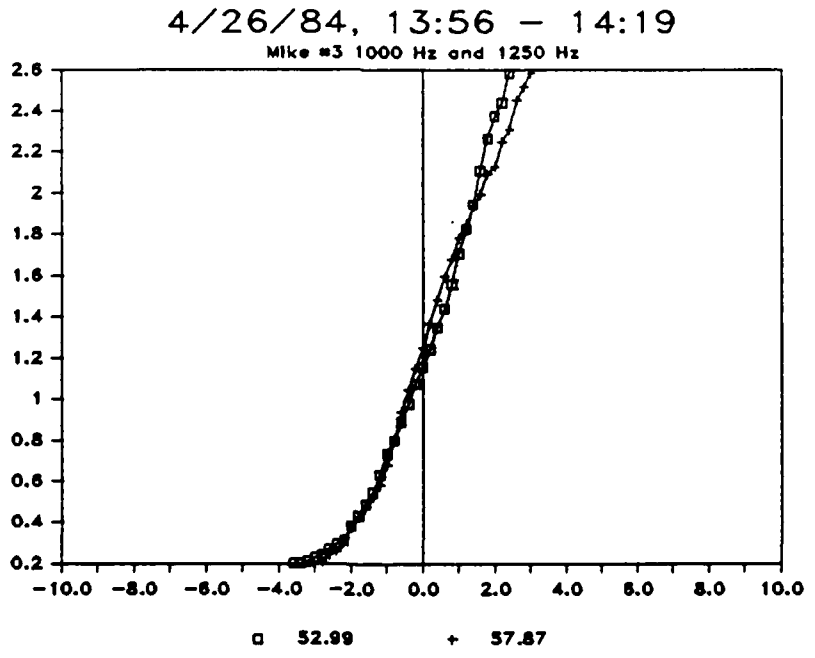

Figure 27: 2 Meter Height, 60 Meter Range

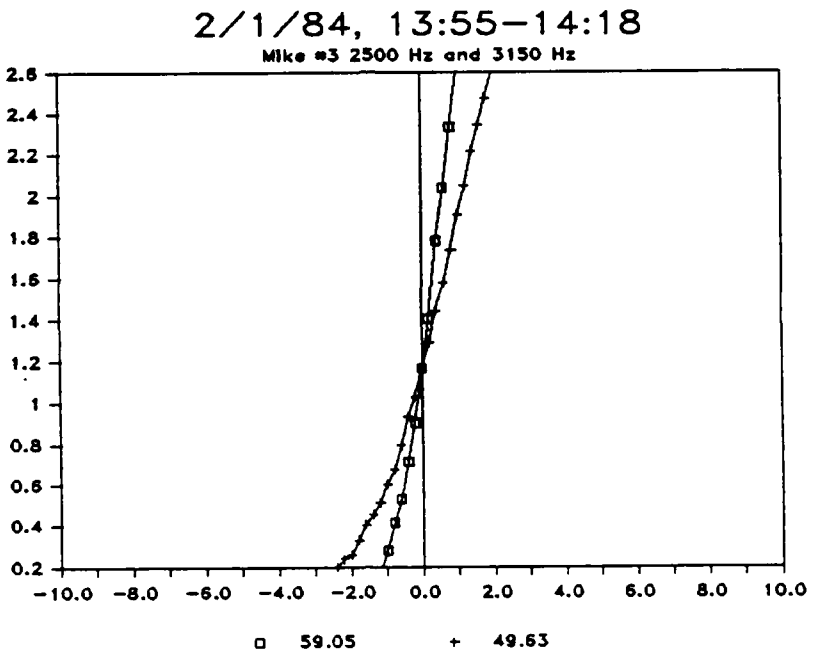

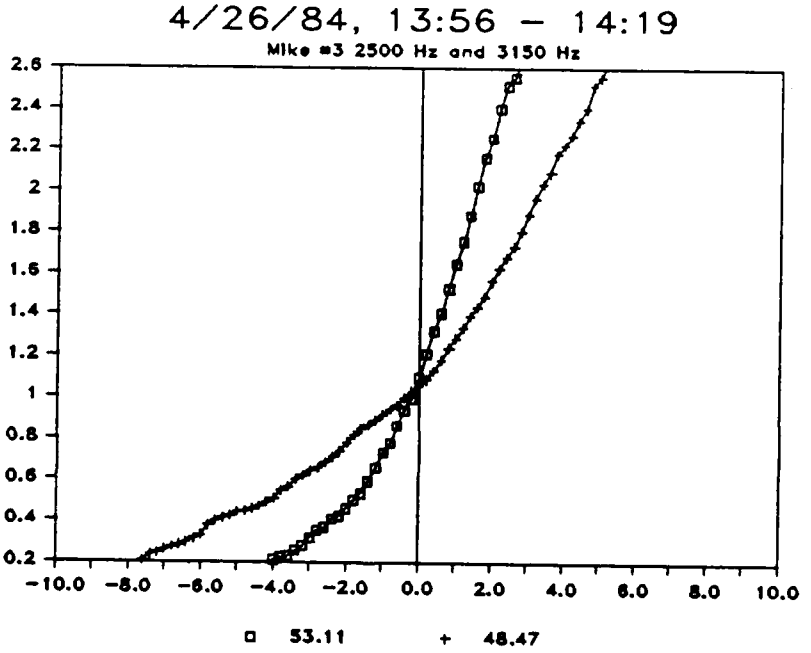

Figure 28: 2 Meter Height, 60 Meter Range

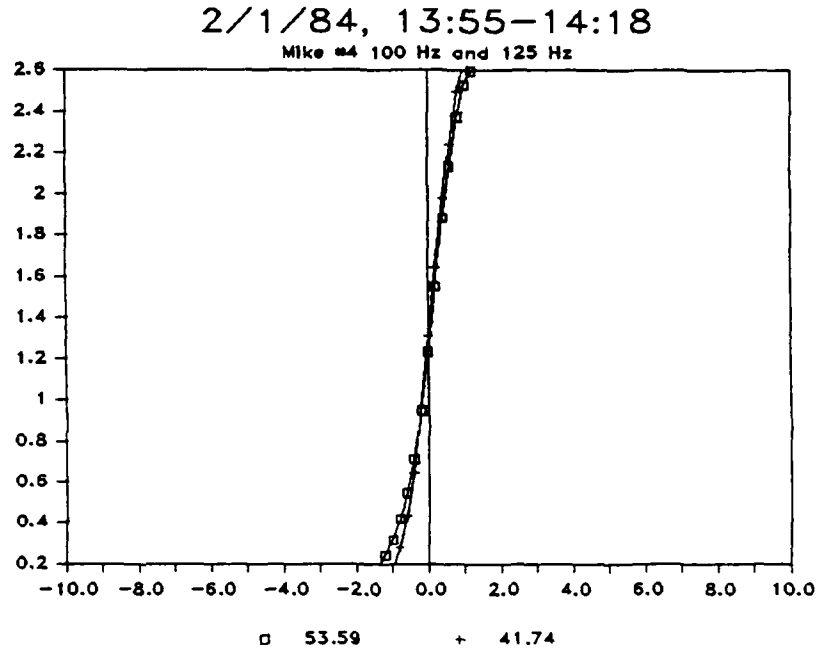

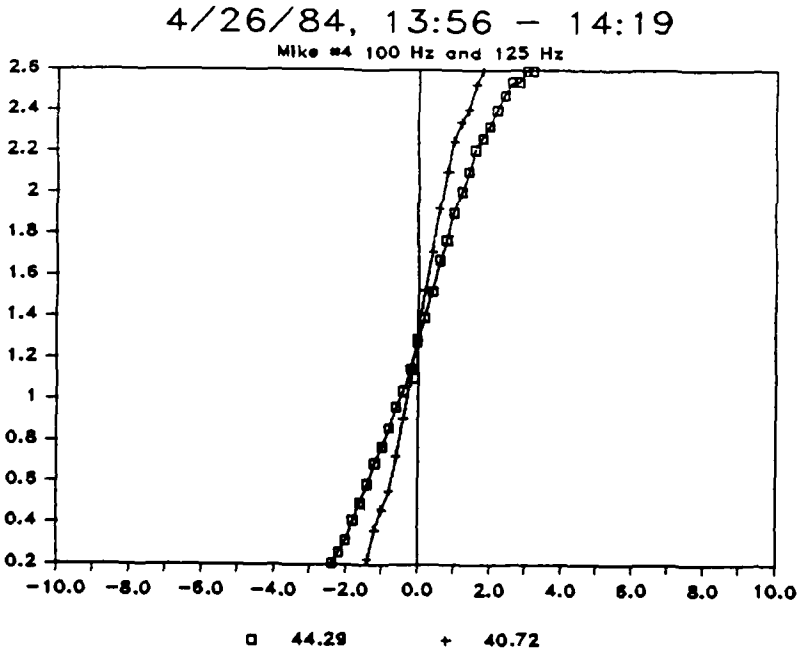

Figure 29: .5 Meter Height, 120 Meter Range

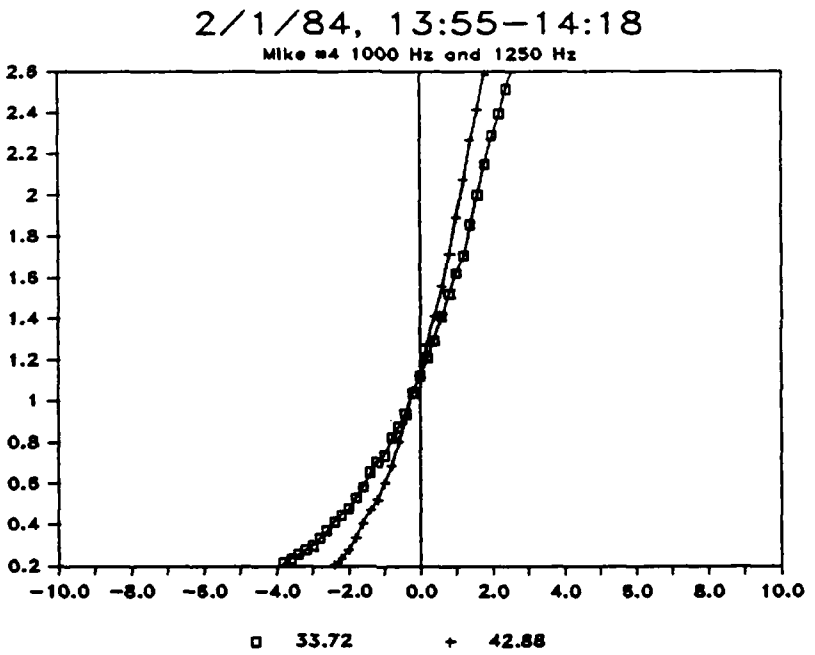

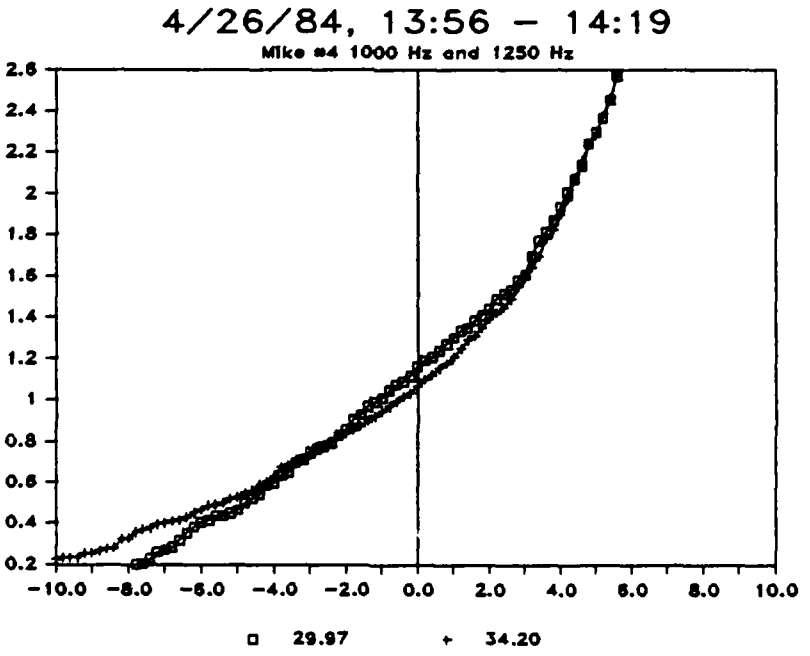

Figure 30: .5 Meter Height, 120 Meter Range

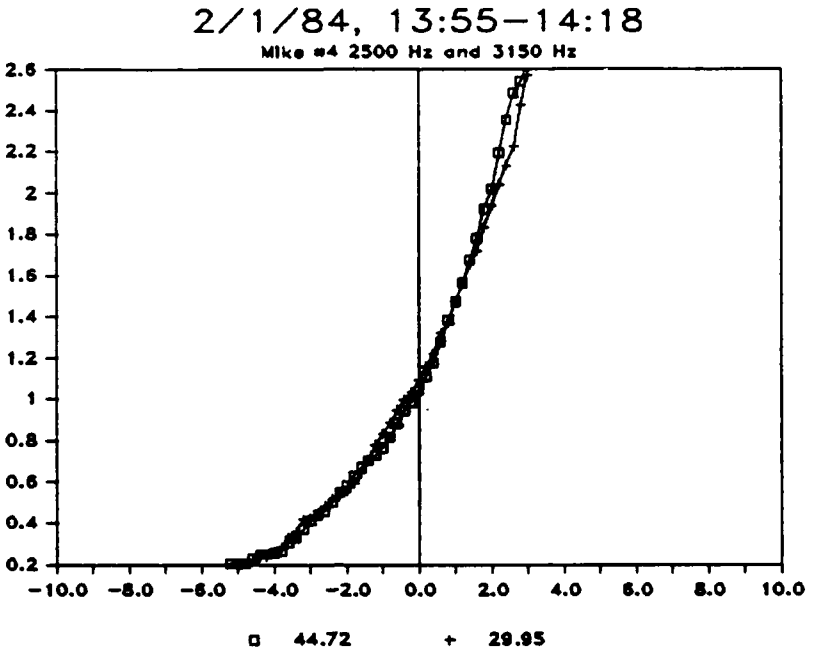

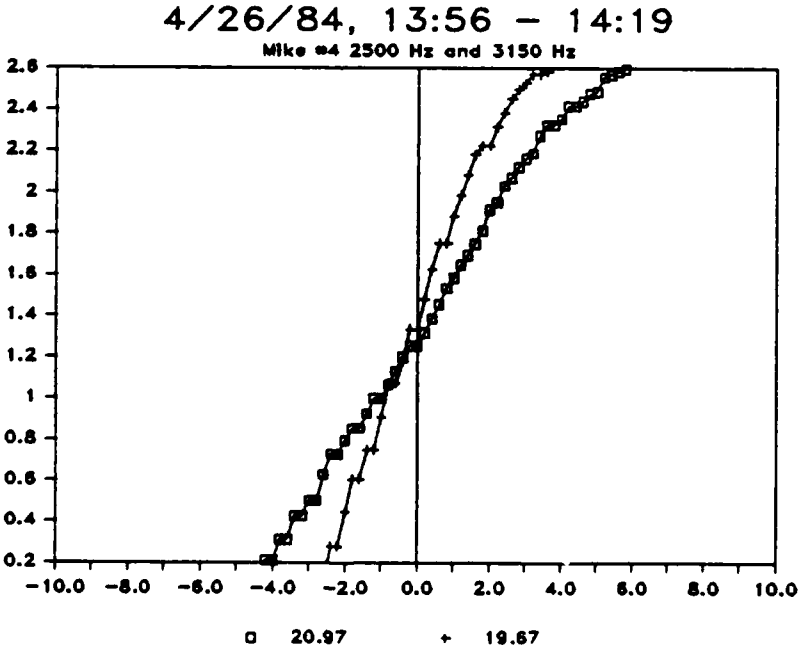

Figure 31: .5 Meter Height, 120 Meter Range

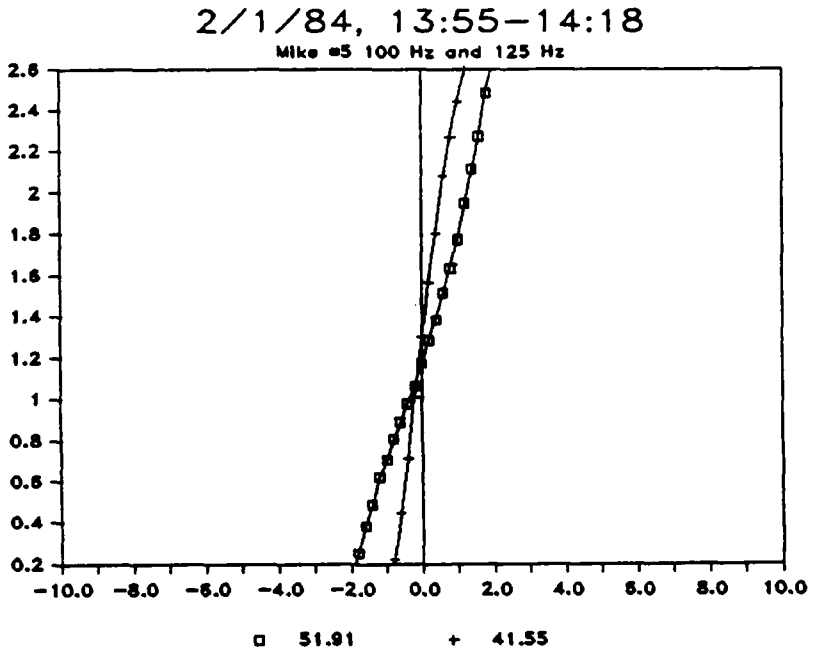

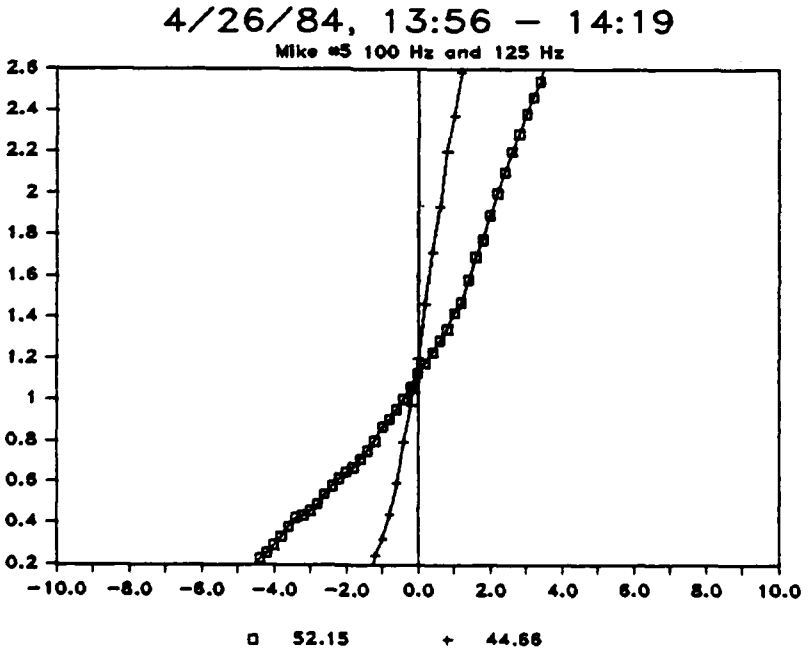

Figure 32: 2 Meter Height, 120 Meter Range

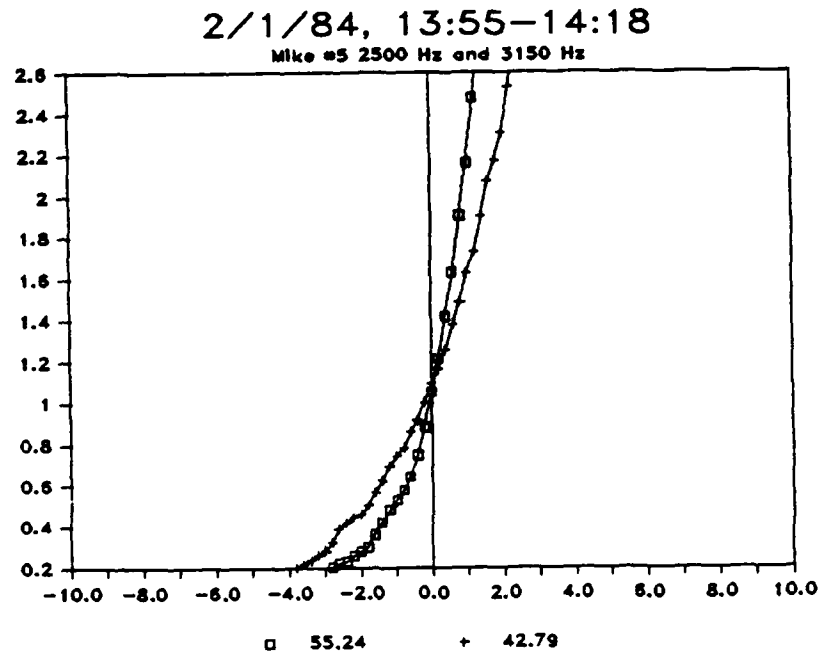

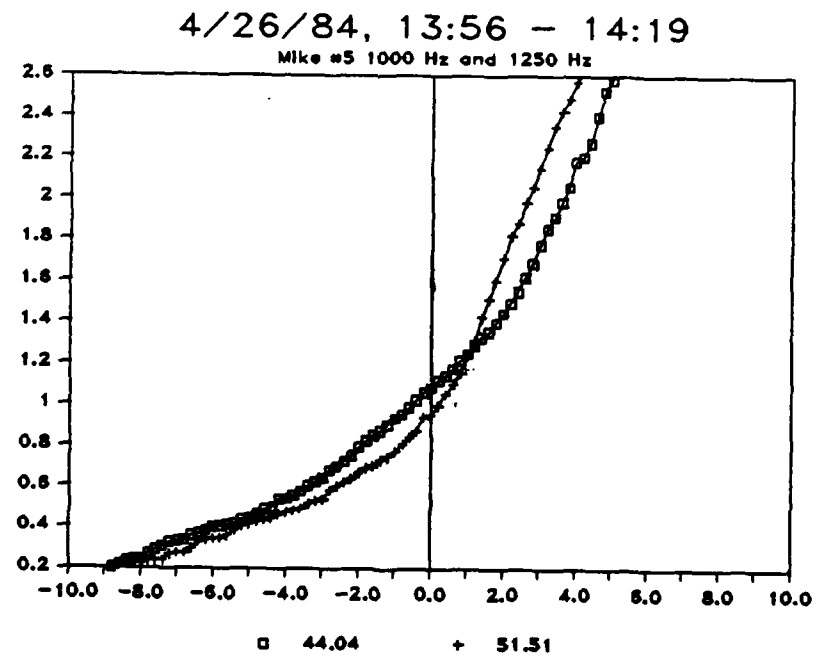

Figure 33: 2 Meter Height, 120 Meter Range

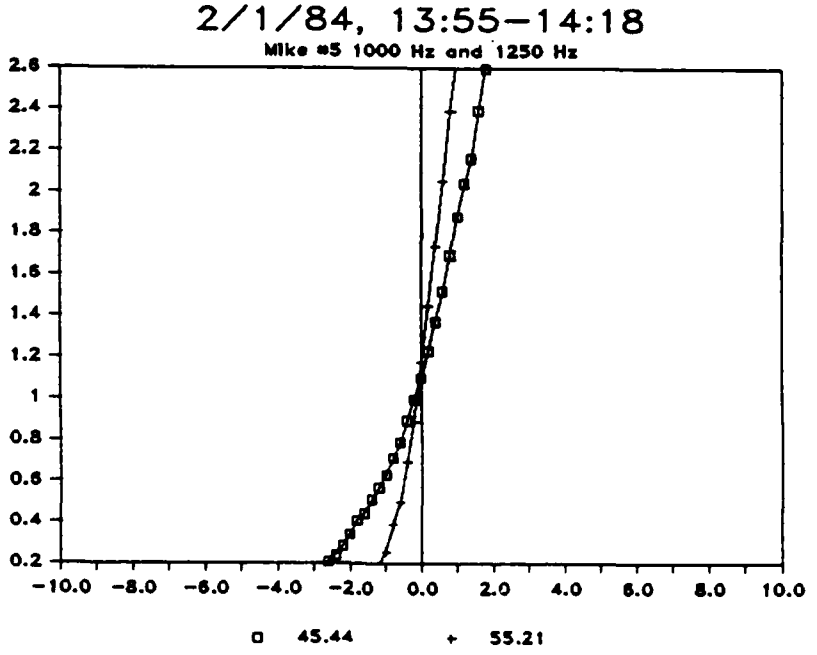

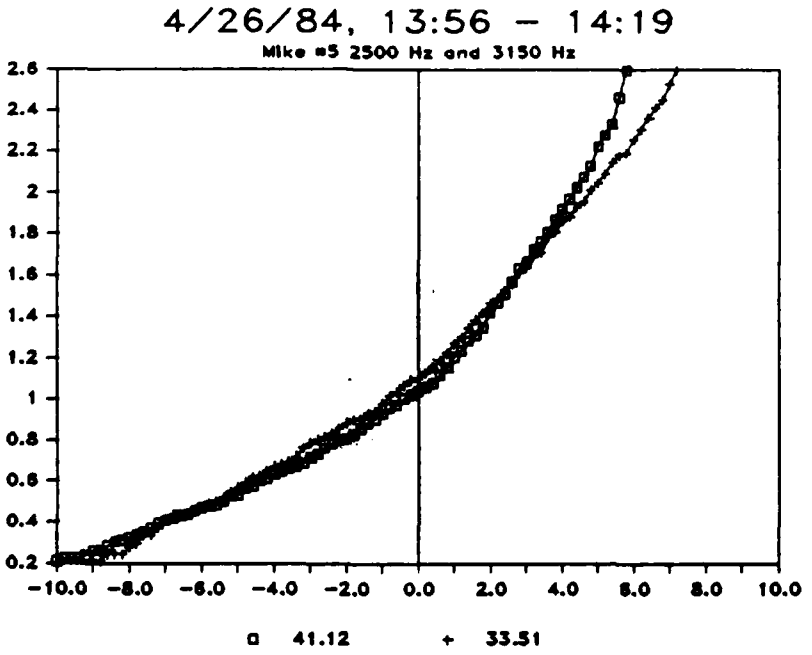

Figure 34: 2 Meter Height, 120 Meter Range

5. Some Preliminary Results and Conclusions

It was evident from the scaled time series of received power at each frequency that the variability above the snow and ground, respectively, of the various tones was visually different to varying degrees at the different transmitted frequencies (see figures 8 through 19). Some of the analyzed cumulative probability density functions derived from such time series are shown in Figures 20 through 34.

Table 2 summarizes the difference in width (corresponding to the statistics of the "depth" of fading) between the fading distributions analyzed in February and April as a function of frequency and path length. With the exception of the 1250 Hz signal at 30 m distance, the width of each fading distribution in April exceeded the corresponding one measured in February. Thus, from statistical analysis of the entire available data set, it may be possible to infer relationships between the magnitude of the sensible heat flux and depth of fading of sound pressure level fluctuations. Note, however, that the observed distributions also clearly show that even in the highly stable, minimum turbulence environment above snow that the received signal at path lengths somewhere in excess of 30 m and at frequencies in excess of 2500 Hz is still fading significantly.

This suggests, first of all, that the atmosphere is probably not sufficiently horizontally homogeneous to justify indiscriminate use of one-dimensional (vertical gradient only) ray theory models. In order to establish the length scales for the turbulent variations of sound speed in the surface layer, and, hence, the distances as a function of height and stability over which horizontal homogeneity might be assumed, it will be necessary to define either theoretically or experimentally the longitudinal vertical and lateral (with respect to the mean flow) coherence functions for the velocity

Table 2. Differential (April-February) Width in dB of Selected Fading Distributions as a Function of Frequency and Path Length

Trans. Height		0.5	2.0	0.5	2.0	0.5	2.0
Frequency		100	125	1000	1250	2500	3150
Distance	30m	1.5	1.0	2.2	(2.5)[1]	4.2	6.9
	60m	3.6	2.4	3.6	3.5	4.6	8.3
	120m	4.0	0.4[2]	9.5	11.0	11.7	10.1

[1] Single case in which February width exceeded April

[2] Sufficiently different to require special analysis

of sound. To this end at least in some cases, because the fluctuations in velocity of sound depend principally upon turbulent wind velocity fluctuations, it may be possible to extend the results of work such as that reported by Kristensen (1979) and Kristensen and Jensen (1979). However, in conditions such as above snow when the temperature gradients are also extremely large, to the authors' knowledge, there is neither a model nor data base which can be used to define the needed properties of the SL acoustic refractive index structure.

Secondly, if it can be shown that the atmospheric refractive index fluctuations are sufficiently small to allow the application of ray theory models, it is essential that attention be given to determining more precisely the geometry of the various ray paths which contribute to the received signal. In particular, application of two or three component (midpath surface reflected, 1 or 2 atmospheric, etc.) ray models simply does seem to be justifiable given the accumulating evidence to the effect that more than half of the surface between the transmitter and receiver is likely to be contributing surface-reflected energy (see e.g., Roth, 1983). If and when multiple surface reflections are important, then the differential grazing angles of various rays will also be of potential importance.

Finally, because the refractive index gradient in the lowest one-half meter of the SL is both largest and most variable with respect to height and time (Thomson and McDaniel, 1985), the refractive index can change substantially over distances corresponding to a wavelength. This being the case, wave rather than ray theory may be required in order to analyze the characteristics of the forward "scattered" energy. During the interpretation of the field data the potential importance of the near surface gradients became apparent. The results of this study show that, in furture studies,

velocity and temperature gradients near the surface should be given careful consideration.

6. Summary of Continuing Work

A draft of a scientific paper for submission to the Journal of the Acoustic Society of America is nearly completed. It is to be titled "The Micrometeorology of Atmospheric Sound Propagation". When completed, data analysis is still in progress, it will have the most complete demonstration of the importance of micrometeorological processes on the definition of the near surface acoustic propagation medium which has ever been complied. For example, the illustrations in progress, which are an extension of the concepts first presented in our 1985 New Orleans paper, emphasize definition of the space-time variability of the propagation-related micrometeorological variables. The experimental data utilized in the preparation of this paper have for the most part been derived from this measurement program.

Completion of the above paper has been delayed as a consequence of the need to substantially upgrade our available computer programs for ray tracing to allow for better treatment of surface "reflections". This work is now nearly completed and the revised software will be applied at the first opportunity to the data base compiled in this program.

Finally, the cumulative distribution functions presented in this report represent only the first step in the total analysis which is possible. Table 3 gives a summary of archived measurements. Recall that the total data base consists of 24 frequencies times, at least, 16 runs times 3 distances. That is, for example, more than 1000 cumulative probability density functions. Hence, we are now atempting to determine some new (and optimal) methods for statistically summarizing the available data. Two of the simpler summaries which are in process include signal variability as a function of frequency and range. However, in each case analysis cannot be completed without careful definition of the exact micrometeorological conditions during each "run".

Table 3. Summary of Archived Measurements

	Run	Start	Stop
1 February 1984	1	11:53	12:35
	2	13:55	14:30
	3	15:30	15:45
	4a	16:15	16:30
	4b1	17:15	17:30
	4b2	17:55	17:59
	5	18:38	19:00
2 February 1984	6	07:20	07:35
	7	08:00	08:31
	9	11:00	11:15
26 April 1984	0	11:40	12:10
	1	13:56	14:20
	2	16:14	16:23
	1 (Reel 4)	18:10	
	2	19:18	19:36

Experimental values such as the "anomolous" 0.4 dB at 125 Hz and 120 m in Table 2 appear to be real. From a statistical point-of-view such points are "outliers". But unless we can establish that the equipment was not working, they must be considered real and thus require individual, time consuming analysis. For example, such points might be the result of caustics which we know are present in such line-of-sight, SL propagation paths. It may be that the mere existence of such data points will provide new insight into the nature of the propagation medium.

7. References

Delany, M. E., (1977), Sound Propagation in the Atmosphere: A Historical Review, Acustica, 38, pp. 201-233.

Hasebe, M., (1983), Sound propagation along a snow surface, J. Acous. Soc. Japan, 4, pp. 211-212.

Kristensen, L., (1979), On Longitudinal Spectral Coherence, Boundary-Layer Meteo., 16, pp. 145-153.

Kristensen, L., (1979), Lateral Coherence in Isentropic Turbulence and in the Natural Wind, Boundary-Layer Meteo., 17, 353-373.

Nicholas, J., J.-L. Berry and G. A. Daigle (1985), Propagation of sound above a finite layer of snow, J. Acous. Soc. Amer., 77, pp. 67-73.

Oke, T. R., (1978), Boundary Layer Climates, Methuen & Co., New York, pp. 68-80.

Piercy, J. E., T. F. W. Embleton and L. C. Sutherland, (1977), Review of Noise Propagation in the Atmosphere, J. Acous. Soc. Amer., 61, pp. 1403-1418.

Roth, S. D., (1983), Acoustic Propagation in the Surface Layer under Convectively Unstable Conditions, Ph.D. Thesis, The Pennsylvania State University, University Park, PA 16802.

Sutherland, L. C., J. E. Piercy, H. E. Bass and L. B. Evans (1974), A Method for Calculating the Absorption of Sound by the Atmosphere, Preprint Inv. Paper Acous. Soc. Amer., St. Louis, MO, 4-8 Nov., 1974.

Thomson, D. W., and O. H. McDaniel, (1985), Recent Progress in Analyzing and Modeling Surface Layer Sound Propagation, Proc. 2nd Symposium on Long Range Propagation and Seismic/Acoustic Coupling, New Orleans, LA, February, 1985.

Tillotsen, J. G. (1985), Attenuation of Sound over Snow-Covered Fields, Letter in J. Acous. Soc. Amer., 20, pp. 846-848.

END

10-86

DTIC